Mathematical Biosciences 258 (2014) 113–133

Contents lists available at ScienceDirect

Mathematical Biosciences

journal homepage: www.elsevier.com/locate/mbs

A new general analytical approach for modeling patterns of genetic differentiation and effective size of subdivided populations over time

Ola Hössjer[a,*], Fredrik Olsson[a], Linda Laikre[b], Nils Ryman[b]

[a] Department of Mathematics, Division of Mathematical Statistics, Stockholm University, SE 106 91 Stockholm, Sweden
[b] Department of Zoology, Division of Population Genetics, Stockholm University, SE 106 91 Stockholm, Sweden

ARTICLE INFO

Article history:
Received 23 November 2013
Revised 9 September 2014
Accepted 7 October 2014
Available online 20 October 2014

2000 MSC:
92D25
60F99

Keywords:
Effective population size
Coefficient of gene differentiation
Matrix analytic methods
Subpopulation weights
State space reduction

ABSTRACT

The main purpose of this paper is to develop a theoretical framework for assessing effective population size and genetic divergence in situations with structured populations that consist of various numbers of more or less interconnected subpopulations. We introduce a general infinite allele model for a diploid, monoecious and subdivided population, with subpopulation sizes varying over time, including local subpopulation extinction and recolonization, bottlenecks, cyclic census size changes or exponential growth. Exact matrix analytic formulas are derived for recursions of predicted (expected) gene identities and gene diversities, identity by descent and coalescence probabilities, and standardized variances of allele frequency change. This enables us to compute and put into a general framework a number of different types of genetically effective population sizes (N_e) including variance, inbreeding, nucleotide diversity, and eigenvalue effective size. General expressions for predictions (g_{ST}) of the coefficient of gene differentiation G_{ST} are also derived. We suggest that in order to adequately describe important properties of a subdivided population with respect to allele frequency change and maintenance of genetic variation over time, single values of g_{ST} and N_e are not enough. Rather, the temporal dynamic patterns of these properties are important to consider. We introduce several schemes for weighting subpopulations that enable effective size and expected genetic divergence to be calculated and described as functions of time, globally for the whole population and locally for any group of subpopulations. The traditional concept of effective size is generalized to situations where genetic drift is confounded by external sources, such as immigration and mutation. Finally, we introduce a general methodology for state space reduction, which greatly decreases the computational complexity of the matrix analytic formulas.

1. Introduction

Determining the amount of genetic variation within and between populations and the rate of loss of genetic variation is of fundamental importance in evolutionary and conservation genetics, and crucial parameters in this respect include the genetically effective population size (N_e) and the coefficient of gene differentiation (G_{ST}). Nei [64] introduced G_{ST} as a multiallelic and multilocus extension of the fixation index F_{ST} of Wright [115,116] and it quantifies the proportion of genetic variation that is explained by genetic differences between populations. The effective size is the size of an ideal homogeneous population without mutations or selection, that has the same expected change of some genetic characteristic (e.g. inbreeding) per generation as the studied one. Many versions of N_e have been developed since the concept was first introduced by Wright [113,114], as reviewed e.g. by Ewens [21], Crow and Denniston [17], Orrive [76], Caballero [7], Wang and Caballero [103], Waples [107], and Charlesworth [11]. Over the years, N_e has become an indispensable tool in conservation biology for identifying population sizes necessary for short and long term conservation of e.g. endangered species and populations [2,27,93,96].

Most models for N_e refer to a single population of constant size, and rules of thumb in conservation genetics are often based on such models assuming single, isolated populations [1]. In real life, however, populations are rarely isolated but are subject to gene flow among more or less isolated subpopulations of varying size that are dispersed over a particular geographic area.

The main purpose of the present paper is to develop theoretical means for assessing effective population size and genetic divergence in a situation with substructured populations that consist of various numbers of more or less interconnected subpopulations whose size can vary over space and time. Specifically, this analytical work was prompted by a practical, real life case – the conservation genetic situation of the Swedish wild wolf population. The Swedish wolf

* Corresponding author. Tel.: +46 70 672 12 18.
E-mail addresses: ola@math.su.se (O. Hössjer), fredriko@math.su.se (F. Olsson), Linda.Laikre@popgen.su.se (L. Laikre), Nils.Ryman@popgen.su.se (N. Ryman).

http://dx.doi.org/10.1016/j.mbs.2014.10.001

population is highly inbred and has been almost completely isolated for several decades. Conservation genetics research has addressed the severe genetic situation (e.g. [46,52,80]), specifically stressing the need for breaking isolation and creating an interconnected population system where the Swedish wolf population can exchange genes with the Finnish population and populations further east [29,47]. Politicians and managers have now also realized this need and various ways of creating gene flow are discussed [53]. However, the necessary properties of such a substructured population in order to meet conservation genetic goals with respect to rate of inbreeding and genetic drift are unclear, because theory for metapopulation effective population size relevant for practical situations such as the current one has been missing. In this paper, we develop the mathematical framework for addressing such issues and several steps are involved in this process, including 1) generalized recursion formulas for a number of genetic quantities, 2) new analytical tools for reporting the time dynamics of N_e and forecasts of G_{ST}, 3) a novel class of subpopulation weights, 4) a generalized unified theory of different types of effective size N_e, and 5) a novel method of computational reduction for populations with symmetries.

We briefly describe these five contributions. First, we consider a class of diploid, monoecious populations evolving in discrete generations under selective neutrality, with mutations, migration and genetic drift (due to random sampling of genes when a finite population reproduces) as evolutionary forces affecting the amount of genetic variation. Whereas formulas for N_e and G_{ST} are often developed under a variety of assumptions, such as a large population, a small migration rate between subpopulations, or a long time frame, we will rather use matrix analytic methods [10] in order to define exact linear recursions for a number of quantities, including identity by descent and coalescence probabilities, standardized variances of allele frequency change, and predicted (expected) gene identities/gene diversities. All these recursions are very similar, with matrices that have rows and columns indexed by pairs of subpopulations. Although several authors have considered such recursions, starting with the seminal work in [56], our setup is more general in that we allow the demographics, in terms of migration patterns, local census and local effective sizes to vary in an arbitrary way, including global and local bottlenecks, subpopulation extinction and recolonization, cyclic changes, or exponential growth. From these recursions we get novel and exact expressions of predictions of G_{ST} and various types of N_e (inbreeding, variance, nucleotide diversity, eigenvalue).

Second, it is essential for protection of genetic characteristics of populations and species to know the rate of loss of genetic variability and subpopulation differentiation over short *and* long time intervals. For a subdivided population it is typically not possible to summarize this information with just a few parameters, not even when the subpopulation census sizes are constant over time. When a population is isolated its degree of inbreeding, for example, will increase at a fixed rate so that N_e is constant from one generation to the next. In contrast, if a subpopulation of a population system receives migrants from the rest of the system, then the rate of inbreeding, and thereby N_e, will vary over time. As a consequence, N_e of the whole system will fluctuate as well, as we will see below. For this reason we generalize a new approach initiated in [73] for age structured models and variance effective sizes, and report N_e as a *function* of the time interval under which genetic loss takes place. Similarly, the predicted G_{ST} depends on when the forecast is made, and it can therefore be computed as a function of the distance between the present and the time point of prediction. This enables researchers to investigate the predicted genetic effects of various demographic scenarios and management schemes that include population systems rather than single, isolated populations.

Third, we consider a large and novel class of schemes of weighting subpopulations and show how they influence N_e and predictions of G_{ST}. Of particular interest are weights that are uniform (all subpopulations weighted equally), proportional to subpopulation sizes (each individual weighted equally) or reproductive (each individual weighted proportionally to its predicted or expected long term number of descendants). We also consider local schemes for which only subsets of subpopulations are assigned positive weights. This could be of interest in practical management when the population managed in a particular area is genetically connected to one or several other populations, which act as more or less known 'ghost populations' [4,91]. For such local weights, it is possible to quantify exactly how various migration scenarios between the population of interest and the other subpopulations affect G_{ST} and N_e.

Fourth, in an influential paper Whitlock and Barton [110] showed that several notions of effective size are closely related for subdivided populations, and here we extend their results by considering time intervals of arbitrary length, and a larger class of effective sizes. To this end, we utilize that each type of effective size involves a quantity that is either defined backwards (identity by descent and coalescence probabilities) or forwards (predicted gene identity, standardized variance of allele frequency change) in time, and the matrices of the corresponding linear recursions can be described in terms of pairs of genes, drawn with or without replacement from the population. Although the latter distinction has a negligible effect for a population with a size of order, say, 100 or larger, it makes it possible to put all notions of effective size into a unified framework, expressing each one of them as a very explicit function of the initial conditions and matrices of its linear recursion and of the subpopulation weights.

Fifth, we define a general way of exploiting invariance between subpopulations, so that whenever certain symmetry conditions hold, the size of the state space can be reduced from s^2, where s is the number of subpopulations.

In Section 2 we define the population dynamics and specify in particular how migration, genetic drift and mutations enter into the model. Subpopulation differentiation is treated in Section 3 and the various types of effective sizes in Section 4. In Section 5 we consider the special case when local census sizes and migration rates are time independent. This is illustrated with several examples that highlight the importance of reporting N_e and predictions of G_{ST} as functions of time. State space reduction is defined and exemplified in Section 6, a summary and discussion are provided in Section 7, some extensions of the theory and proofs can be found in Appendix A, and finally, Table 1 provides a list of notations for some of the most important quantities of the paper.

2. Model for demographics, reproduction, and mutations

Consider a diploid and monoecious population with a random amount of selfing that is subdivided, with s subpopulations. It evolves in discrete generations $t = \dots, -1, 0, 1, 2, \dots$ of which $t < 0$ represents the past, $t = 0$ the present and $t > 0$ the future. Let $N_{ti} \geq 0$ be the local census size of subpopulation i in generation t, with $N_{ti} = 0$ corresponding to extinction. Each individual carries two copies of a gene, so that the total number of genes in subpopulation i and generation t is $2N_{ti}$. The total census size $N_t = \sum_{i=1}^{s} N_{ti}$ in generation t is assumed to be positive, so that at least one subpopulation is non-extinct.

The local effective size N_{eti} in generation t of subpopulation i is usually (but not necessarily) smaller than or equal to its local census size N_{ti}. The more variable reproduction between individuals in i is, the smaller is N_{eti}.

Occasionally, migration between subpopulations takes place, as quantified by the forward and backward migration rates $M_{t-1,ki}$ and B_{tik} from subpopulation k of generation $t-1$ to subpopulation i of generation t. More precisely, each gene of subpopulation k and generation $t-1$ has an expected number $M_{t-1,ki}$ of offspring, which, in the next generation t, live in subpopulation i, whereas B_{tik} is the probability that a parent of a gene in subpopulation i and generation t originates from subpopulation k in the previous generation $t-1$. The

Table 1
Notation for selected quantities of the paper.

Symbol	Definition
s	Number of subpopulations
N_{ti}	Local census size of subpopulation i in generation t ($= N_i$ if time independent)
N_t	Global census size $\sum_{i=1}^{s} N_{ti}$ of generation t ($= N$ if time independent)
N_{eti}	Local effective size of subpopulation i in generation t
$\boldsymbol{M}_t = (M_{tki})$	Matrix with forward migration rates between all pairs of subpopulations from generation t to $t+1$
$\boldsymbol{B}_t = (B_{tik})$	Matrix with backward migration rates between all pairs of subpopulations from generation t to $t-1$
μ	Mutation probability for each gamete
P_{tia}	Frequency of allele a in subpopulation i of generation t
H_{tij}	Gene diversity between subpopulations i and j of generation t
$\boldsymbol{h}_t = (h_{tij})$	Column vector of s^2 predicted gene diversities between all pairs of subpopulations, generation t
F_{tij}	Gene identity between subpopulations i and j of generation t
$\boldsymbol{f}_t = (f_{tij})$	Column vector of s^2 predicted gene identities between all pairs of subpopulations, generation t, or identity by descent probabilities between generations t_1 and t, or standardized genetic drift covariances between generations 0 and t
$\mathbf{1}$	Column vector of s^2 ones
$\boldsymbol{\delta}_t = (\delta_{tij})$	Column vector of s^2 probabilities of drawing the same gene with replacement from all pairs of subpopulations
$\boldsymbol{A}_t = (A_{tij,kl})$	Square matrix of order s^2 in gene identity with replacement recursions
$\boldsymbol{D}_t = (D_{tij,kl})$	Square matrix of order s^2 in gene identity without replacement recursions
w_i	Weight assigned to subpopulation i
$\boldsymbol{W}_T = (w_i w_j)$	Row vector of s^2 sampling probabilities, all pairs of subpopulations, scheme T
$\boldsymbol{W}_S = (w_i 1_{\{i=j\}})$	Row vector of s^2 sampling probabilities, all pairs of subpopulations, scheme S
u_i	Relative size of subpopulation i (if constant over time)
γ_i	Probability that distant ancestor belongs to subpopulation i (constant migration)
$\mathcal{S}$	Subset of subpopulations that have positive weights
G_{STt}	Coefficient of gene differentiation in generation t
g_{STt}	Predicted G_{STt} based on information from generation 0
$N_{el}(\mathcal{T})$	Inbreeding effective size over time interval $\mathcal{T}$, global when all $w_i > 0$
$N_{e\pi}((-\infty, t])$	Nucleotide diversity effective size based on coalescence time of two genes from generation t, global when all $w_i > 0$
$N_{eV}(\mathcal{T})$	Variance effective size over time interval $\mathcal{T}$, global when all $w_i > 0$
N_{eE}	Eigenvalue effective size, always globally for the whole population
λ	Largest eigenvalue of $\boldsymbol{A}_t = \boldsymbol{A}$ and $\boldsymbol{D}_t = \boldsymbol{D}$
$\boldsymbol{r} = (r_{ij})$	Right eigenvector of $\boldsymbol{A}$ corresponding to eigenvalue λ
$\boldsymbol{\rho} = (\rho_{ij})$	Left eigenvector of $\boldsymbol{A}$ corresponding to eigenvalue λ
$\tilde{\boldsymbol{r}} = (\tilde{r}_{ij})$	Right eigenvector of $\boldsymbol{D}$ corresponding to eigenvalue λ
$\tilde{\boldsymbol{\rho}} = (\tilde{\rho}_{ij})$	Left eigenvector of $\boldsymbol{D}$ corresponding to eigenvalue λ
m	Migration rate, i.e. proportion of offspring that belong to a subpopulation different from their parents
m'	Defined for the island model, $= sm/(s-1)$
NaN	Not a number

forward migration rates determine the time progression of the local census sizes, according to

$$N_{ti} = \sum_{k=1}^{s} N_{t-1,k} \mathcal{M}_{t-1,ki}, \tag{1}$$

where each term on the right hand side gives the number of offspring that the parents in subpopulation k and generation $t-1$ contribute to subpopulation i in generation t. In particular, $\mathcal{M}_{t-1,ki}$ is the observed forward migration rate, a random variable with $E(\mathcal{M}_{t-1,ki}) = M_{t-1,ki}$. In order to define a larger and more flexible class of forward migration rates, we will not always require that $N_{t-1,k}$ and N_{ti} are integers in (1). When $N_{t-1,k} = 0$, the forward rates from subpopulation k in generation $t-1$ are not well defined, and this we write as $\mathcal{M}_{t-1,ki} = M_{t-1,ki} = \text{NaN}$, where NaN is short for 'Not a Number', and a convention $0 \cdot \text{NaN} = 0$ is assumed in (1). However, a subpopulation k that is extinct in generation $t-1$ may still be recolonized in the next generation through migration from *other* subpopulations, as described in (1). The backward rates satisfy

$$B_{tik} = \begin{cases} \dfrac{N_{t-1,k} M_{t-1,ki}}{N_{ti}}, & N_{ti} > 0, \\ \text{NaN}, & N_{ti} = 0. \end{cases} \tag{2}$$

The total number of genetic variants (alleles) in generation t is $n_t \geq 1$, and for any non-extinct subpopulation i in generation t, P_{tia} is the fraction of genes in generation t and subpopulation i carrying allele $a = 1, \ldots, n_t$, whereas $P_{tia} = \text{NaN}$ if $N_{ti} = 0$. Our model of subpopulation extinction and recolonization is very general, but for notation convenience we only consider non-extinct subpopulations in the main text, and refer to the end of Appendix A for the extended theory. See also [32,89,111] for more specific models of subpopulation extinction and recolonization.

The gene is assumed to be selectively neutral, with a mutation probability $0 \leq \mu \leq 1$ per gamete and generation. We will assume an infinite allele model [42], so that each mutation creates a new allele, never seen before. In more detail, the reproduction cycle between generations $t-1$ and t can be summarized in four steps as follows:

1. In each (non-extinct) subpopulation $k = 1, \ldots, s$ of generation $t-1$, a random subset $N_{e,t-1,k}$ of all $N_{t-1,k}$ individuals are selected as breeders. An infinitely sized pre-migration gamete pool k is formed, to which all breeders' genes contribute in equal proportions $1/(2N_{e,t-1,k})$.
2. Migration takes place by exchange of genetic material between gamete pools, so that, after migration gamete pool i of a subpopulation that is non-extinct in generation t, is a mixture of pre-migration gamete pools $1, \ldots, s$ in proportions B_{tik}, $k = 1, \ldots, s$.
3. The gametes of all post-migration pools i of step 2 mutate independently with probability μ.
4. Fertilization in a (non-extinct) subpopulation $i \in \{1, \ldots, s\}$ of generation t proceeds, selecting $2N_{ti}$ gametes randomly from post-migration gamete pool i of step 3, corresponding to N_{ti} diploid individuals.

Since fertilization in step 4 takes place in infinitely sized post-migration pools, the number of genes drawn from each parental

subpopulation have a multinomial distribution, and therefore

$$(2N_{t-1,1}\mathcal{M}_{t-1,1i},\ldots,2N_{t-1,s}\mathcal{M}_{t-1,si}) \sim \text{Mult}(2N_{ti};B_{ti1},\ldots,B_{tis}).$$

Sampson [85] employed a special case of reproduction cycle 1–4 without mutations, identical local effective and census sizes of all subpopulations ($N_{eti}=N_{t1}$), with $(N_{t1},\ldots,N_{ts})$ varying rapidly according to a Markov chain with a finite state space. See also Nagylaki [61], who considered a model similar to 1–4, with equal effective and census sizes of all subpopulations that are constant over time ($N_{eti}=N_{ti}=N_i$), and selection added in a separate step between 1 and 2. For the infinite island model, 1–4 corresponds to a scheme that Sved and Latter [95] referred to as stochastic migration with a stochastic migration rate.

3. Subpopulation differentiation

In this section, we quantify inbreeding in terms of allele frequencies at one single locus, with the goal of obtaining general expressions for how predictions of inbreeding and the coefficient of gene differentiation (G_{ST}) evolve over time, with numerical illustrations in Example 1 of Section 5. In the next section, we will also define inbreeding from identity by descent sharing and coalescence probabilities.

3.1. Gene diversities and identities with replacement

Suppose two genes are drawn randomly from two subpopulations i and j of generation t, with replacement if $i=j$. Following [64,67], we quantify inbreeding by means of the gene identity

$$F_{tij}=\sum_{a=1}^{n_t}P_{tia}P_{tja} \tag{3}$$

between subpopulation i and j in generation t as the probability that the two genes are identical by state (IBS), i.e. have the same allele. The probability that the two alleles are different is referred to as the gene diversity

$$H_{tij}=1-F_{tij}=\sum_{\substack{1\le a,b\le n_t\\ a\neq b}}P_{tia}P_{tjb} \tag{4}$$

of i and j in generation t. When $i=j$, the gene identity and gene diversity are identical to the homozygosity and heterozygosity of subpopulation i, only when the genotype frequencies of i conform with Hardy–Weinberg proportions. Otherwise the concepts are different, since genotype frequencies cannot be determined from the allele frequencies alone.

An advantage of (3)–(4) is that genotype frequencies need not be specified when $i=j$, and that the same definition applies when $i\neq j$. Define

$$\begin{aligned} f_{tij}&=E_0(F_{tij}),\\ h_{tij}&=E_0(H_{tij}),\end{aligned} \tag{5}$$

as expectations conditionally on allele frequencies of the present (index 0 of E corresponding to $t=0$). We regard (5) as predictions of F_{tij} and H_{tij}, given information on allele frequencies from $t=0$, and in particular $f_{0ij}=F_{0ij}$ and $h_{0ij}=H_{0ij}=1-f_{0ij}$. In Appendix A, we show that

$$0\le f_{tij}\le\sqrt{f_{tii}f_{tjj}}, \tag{6}$$

for any pair of subpopulations i and j of generation t.

The predicted gene identities and diversities satisfy linear recurrence relations. In order to formulate these recursions, it is convenient to collect all f_{tij} and h_{tij} of generation t into column vectors $\boldsymbol{f}_t=(f_{tij},\ 1\le i,j\le s)$ and $\boldsymbol{h}_t=(h_{tij}\ 1\le i,j\le s)$ of length s^2, where ij is short-hand notation for column number $(j-1)s+i$. We introduce the $s^2\times s^2$ matrix $\boldsymbol{A}_t=(A_{tij,kl};1\le i,j,k,l\le s)$, whose row and column numbers $(j-1)s+i$ and $(l-1)s+k$ are abbreviated as ij and kl respectively, with elements

$$A_{tij,kl}=\left(1-\frac{1}{2N_{ti}}\right)^{\{i=j\}}B_{tik}B_{tjl}\left(\frac{1-\frac{1}{2N_{e,t-1,k}}}{1-\frac{1}{2N_{t-1,k}}}\right)^{\{k=l\}}. \tag{7}$$

It is shown in Appendix A that

$$\begin{aligned}\boldsymbol{f}_t&=(1-\mu)^2(\boldsymbol{A}_t\boldsymbol{f}_{t-1}-\boldsymbol{A}_t\boldsymbol{1}+\boldsymbol{1})+\left(1-(1-\mu)^2\right)\boldsymbol{\delta}_t,\\ \boldsymbol{h}_t&=(1-\mu)^2\boldsymbol{A}_t\boldsymbol{h}_{t-1}+\left(1-(1-\mu)^2\right)(\boldsymbol{1}-\boldsymbol{\delta}_t),\end{aligned} \tag{8}$$

for $t=1,2,3,\ldots$, where $\boldsymbol{1}$ is a column vector of s^2 ones, and $\boldsymbol{\delta}=(\delta_{tij})$ is another column vector of length s^2 with elements $\delta_{tij}=1_{\{i=j\}}/(2N_{ti})$.

3.2. Gene diversities and identities without replacement

Suppose instead that the two genes of the previous section are required to be distinct, so that they are drawn without replacement when $i=j$. Then the probabilities that the two genes are identical and different by state, are

$$\begin{aligned}F_{tij}&=\begin{cases}\displaystyle\sum_{a=1}^{n_t}P_{tia}\frac{2N_{ti}P_{tia}-1}{2N_{ti}-1}, & i=j,\\ \displaystyle\sum_{a=1}^{n_t}P_{tia}P_{tja}, & i\neq j,\end{cases}\\ H_{tij}&=\begin{cases}\displaystyle\sum_{a\neq b}P_{tia}\frac{2N_{ti}P_{tib}}{2N_{ti}-1}, & i=j,\\ \displaystyle\sum_{a\neq b}P_{tia}P_{tjb}, & i\neq j,\end{cases}\end{aligned} \tag{9}$$

for any pair i,j of subpopulations in generation t. These quantities were studied by Malécot [56], when all local census and effective sizes are identical and constant over time. We refer to (9) as the gene identity and gene diversity of subpopulations i and j in generation t, for genes drawn without replacement. Although Nei [64] used the other definition (3)–(4) when defining G_{ST}, it is implicit from [51], [65, p. 122] and [84] that these authors' expected gene identity recursions employed (9).

It is shown in Appendix A that the predicted gene identity between two *distinct* subpopulations i and j, satisfies the inequality

$$0\le f_{tij}\le\sqrt{\left(\frac{2N_{ti}-1}{2N_{ti}}f_{tii}+\frac{1}{2N_{ti}}\right)\left(\frac{2N_{tj}-1}{2N_{tj}}f_{tjj}+\frac{1}{2N_{tj}}\right)}. \tag{10}$$

The recursions (8) for predicted gene identities/diversities, are modified to

$$\begin{aligned}\boldsymbol{f}_t&=(1-\mu)^2(\boldsymbol{D}_t\boldsymbol{f}_{t-1}-\boldsymbol{D}_t\boldsymbol{1}+\boldsymbol{1}),\\ \boldsymbol{h}_t&=(1-\mu)^2\boldsymbol{D}_t\boldsymbol{h}_{t-1}+\left(1-(1-\mu)^2\right)\boldsymbol{1},\end{aligned} \tag{11}$$

for $t=1,2,3,\ldots$, when genes are drawn without replacement, where $\boldsymbol{D}_t=(D_{tij,kl})$ is an $s^2\times s^2$ matrix with elements

$$D_{tij,kl}=B_{tik}B_{tjl}\left(1-\frac{1}{2N_{e,t-1,k}}\right)^{\{k=l\}}. \tag{12}$$

We may interpret (12) as a non-coalescence probability of two distinct genes sampled from i and j in generation t, given that their parents reside in k and l. The explicit solution of the upper part of (11);

$$\begin{aligned}\boldsymbol{f}_t&=(1-\mu)^{2t}\boldsymbol{D}_t\cdot\ldots\cdot\boldsymbol{D}_1\boldsymbol{f}_0\\ &\quad+\sum_{\tau=1}^{t}(1-\mu)^{2(t-\tau+1)}\boldsymbol{D}_t\cdot\ldots\cdot\boldsymbol{D}_{\tau+1}(\boldsymbol{1}-\boldsymbol{D}_\tau\boldsymbol{1})\\ &\overset{\mu=0}{=}\boldsymbol{1}-\boldsymbol{D}_t\cdot\ldots\cdot\boldsymbol{D}_1(\boldsymbol{1}-\boldsymbol{f}_0),\end{aligned} \tag{13}$$

extends a formula of [65] for a single ($s=1$) population.

3.3. Defining sampling probabilities

We will define two different schemes for sampling a pair of genes from the global population. This sampling is a theoretical construct, needed to define a number of quantities below, and should not be confused with collecting real data and estimating parameters. The two schemes we propose are hierarchical, where in the first step, a pair of subpopulations is selected, and in the second step, a pair of genes is sampled from the selected pair of subpopulations (as described in the previous section). In order to formalize the first step, we introduce a vector of non-negative subpopulation weights $\boldsymbol{w}_t = (w_{t1}, \ldots, w_{ts})$ that sum to one, i.e. $\sum_{i=1}^{s} w_{ti} = 1$. Unless otherwise stated, we will assume that the weight vector $\boldsymbol{w}_t = \boldsymbol{w} = (w_1, \ldots, w_s)$ does not change with time, although this is not required for all formulas. For instance, if $\mathcal{S} \subset \{1, \ldots, s\}$ is a fixed subset of subpopulations from which we plan to collect genetic data, a possible weighting scheme is

$$w_i = \frac{1_{\{i \in \mathcal{S}\}}}{|\mathcal{S}|}, \tag{14}$$

where $|\mathcal{S}|$ refers to the number of subpopulations included in $\mathcal{S}$, whereas the remaining $s - |\mathcal{S}|$ ghost subpopulations are only included in the analysis indirectly, through migration. If samples are taken from all subpopulations ($\mathcal{S} = \{1, \ldots, s\}$) formula (14) reduces to uniform weights

$$w_i = \frac{1}{s}. \tag{15}$$

The two sampling schemes are defined as follows:

Sampling scheme T: Select a pair of subpopulations with probability $w_i w_j$, $1 \le i, j \le s$. Then sample two genes, one from each of i and j.
Sampling scheme S: Select a subpopulation with probability w_i, $i = 1, \ldots, s$. Then sample two genes from the chosen subpopulation i.

Whereas the first sampling scheme quantifies genetic variation of the total (T) set of subpopulations with positive weights, the second one quantifies genetic variation within these subpopulations (S).

If two genes are sampled in generation t, their gene identities/diversities for each of the two sampling schemes are

$$\begin{aligned} F_{Tt} &= \sum_{i,j=1}^{s} w_i w_j F_{tij}, \\ F_{St} &= \sum_{i=1}^{s} w_i F_{tii}, \\ H_{Tt} &= 1 - F_{Tt} = \sum_{i,j=1}^{s} w_i w_j H_{tij}, \\ H_{St} &= 1 - F_{St} = \sum_{i=1}^{s} w_i H_{tii}, \end{aligned} \tag{16}$$

with F_{tij} and H_{tij} formulated with or without replacement, as in (3)–(4) and (9). When uniform subpopulation weights (15) are used and the genes are drawn with replacement, (16) equals the definitions of the gene identity and gene diversity in Section 6.4 of [65].

3.4. Coefficient of gene differentiation

In order to assess how genetically different the subpopulations are, we use the coefficient of gene differentiation

$$G_{STt} = G_{STt}^{\boldsymbol{w}} = \frac{F_{St} - F_{Tt}}{1 - F_{Tt}} = \frac{H_{Tt} - H_{St}}{H_{Tt}} \tag{17}$$

of generation t. This quantity was introduced by Nei [64,66], first for uniform (15) and then for more general weighting schemes. It is assumed that the two genes are drawn with replacement in (17), in order to guarantee that G_{STt} is non-negative, see Appendix A for details.

For a future ($t > 0$) generation, $G_{STt}^{\boldsymbol{w}}$ is unknown, with a certain distribution depending on the random nature of genetic drift, migration, and mutation. A single value forecast $g_{STt}^{\boldsymbol{w}}([0, t])$ should approximate some central point (median, expected value, ...) of the predictive distribution of $G_{STt}^{\boldsymbol{w}}$ over time interval $[0, t]$. One such quantity

$$g_{STt} = g_{STt}^{\boldsymbol{w}}([0, t]) = \frac{E_0(F_{St} - F_{Tt})}{E_0(1 - F_{Tt})} = \frac{f_{St} - f_{Tt}}{1 - f_{Tt}} \tag{18}$$

was introduced by Nei [65] and further studied in [68]. It employs the predicted (or expected) gene identities

$$\begin{aligned} f_{Tt} &= E_0(F_{Tt}) = \sum_{i,j=1}^{s} w_i w_j f_{tij}, \\ f_{St} &= E_0(F_{St}) = \sum_{i=1}^{s} w_i f_{tii}, \end{aligned} \tag{19}$$

of sampling schemes T and S respectively in generation t.

Let $\boldsymbol{W}_T = (w_i w_j;\ 1 \le i, j \le s)$ and $\boldsymbol{W}_S = (1_{\{i=j\}} w_i;\ 1 \le i, j \le s)$ be row vectors of length s^2, whose elements are weights assigned by sampling schemes T and S to all pairs of subpopulations. We can reexpress (18) as

$$g_{STt} = \frac{(\boldsymbol{W}_S - \boldsymbol{W}_T)\boldsymbol{f}_t}{1 - \boldsymbol{W}_T \boldsymbol{f}_t}, \tag{20}$$

with $\boldsymbol{f}_t$ computed from the upper recursion of (8) when genes are drawn with replacement. If f_{tii} has been specified within all subpopulations, it follows from (6) that the maximal value of g_{STt} has $f_{tij} = 0$ for all distinct pairs $i \ne j$ [31]. One may also define versions of G_{STt} and g_{STt} with genes drawn without replacement, using the upper recursion of (11) in (20). However, this is less appropriate, since G_{STt} then becomes negative when the frequencies of any allele is the same in all subpopulations.

4. Effective population sizes

In this section we examine the inbreeding (N_{eI}), nucleotide diversity ($N_{e\pi}$), variance (N_{eV}) and eigenvalue (N_{eE}) effective sizes, with a notation

$$N_{eX}(\mathcal{T}) = N_{eX}^{\boldsymbol{w}}(\mathcal{T}), \tag{21}$$

for $X \in \{I, \pi, V, E\}$, where $\mathcal{T}$ is a finite or infinite time interval and $\boldsymbol{w}$ a vector of subpopulation weights. Eq. (21) quantifies the expected loss of genetic variability due to changed allele frequencies, in those subpopulations that have positive weights w_i, per generation during $\mathcal{T}$. These allele frequency changes are not only caused by genetic drift, but confounding effects of migration and mutation could also be present. Throughout this section we assume $\mu = 0$, so that only genetic drift and migration will influence N_{eX}. In particular, if the subpopulations within $\mathcal{S}$ have positive weights (cf. (14)), migration between $\mathcal{S}$ and its complement will influence N_{eX} as a confounder, as shown explicitly in [83] for the island model.

4.1. Inbreeding effective size

In the original definition of the inbreeding effective size N_{eI} in [113], two genes are drawn without replacement from a population, and the probability is derived that their parental genes are from the same individual. We generalize this definition of N_{eI} to structured populations in the context of reproduction model 1–4 of Section 2, where the probability of having the same parent is twice the probability of having identical parental genes. Our generalization includes longer time intervals than one single generation that may extend not

only backwards, but also forwards in time, and genes may be sampled with and without replacement, see Examples 3–5 of Section 5 for numerical illustrations.

Two gene copies are either IBD if they originate from the same mutated allele; under the infinite allele model, this is equivalent to being IBS. Alternatively, two alleles are IBD if they originate from the same ancestral gene of a founder generation $t_0 \le 0$. We employ the second IBD definition, so that each individual of the founder generation contributes with two IBD classes. We let $\mathcal{P}_{tic}$ be the frequency of IBD class $c = 1, \ldots, 2N_{t_0}$ in subpopulation i of generation $t \ge t_0$. In absence of mutations ($\mu = 0$), these IBD frequencies determine allele frequencies through

$$P_{tia} = \sum_{c \in \mathcal{C}_a} \mathcal{P}_{tic},$$

where $\mathcal{C}_a \subset \{1, \ldots, 2N_{t0}\}$ is the set of IBD classes with allele a. In particular $P_{tic} = \mathcal{P}_{tic}$ if all alleles of the founder generation are different.

4.1.1. Drawing without replacement

When two genes are drawn without replacement from i and j at time t, they have a probability

$$\mathcal{F}_{tij} = \begin{cases} \sum_{c=1}^{2N_{t_0}} \mathcal{P}_{tic} \dfrac{2N_{ti}\mathcal{P}_{tic} - 1}{2N_{ti} - 1}, & i = j, \\ \sum_{c=1}^{2N_{t_0}} \mathcal{P}_{tic}\mathcal{P}_{tjc}, & i \ne j, \end{cases} \tag{22}$$

of being IBD. For two generations t_1 and t satisfying $t_0 \le t_1 \le t$, we let

$$f_{tij} = f^{\mathrm{IBD}}_{t_1 tij} = E_{t_1}(\mathcal{F}_{tij}) \tag{23}$$

be the forward predicted IBD probability of two genes of subpopulations i and j at generation t, given that the sizes of all IBD classes are known at time t_1. An equivalent backward in time interpretation of f_{tij} is the probability that the two genes will have ancestors from generation t_1 that are IBD, given that we know the IBD classes at that time.

Let $\boldsymbol{f}_t = \boldsymbol{f}^{\mathrm{IBD}}_{t_1 t}$ be a column vector of length s^2 containing all IBD probabilities f_{tij}. Since our IBD definition does not involve mutations, $\boldsymbol{f}_{t_1}, \boldsymbol{f}_{t_1+1}, \ldots$ satisfy the upper recursion of (11) with $\mu = 0$ and initial condition $\boldsymbol{f}_{t_1}$. From (13) (with 0 replaced by t_1) we derive the IBD probability of two genes, chosen randomly without replacement with scheme T from generation t, as

$$\begin{aligned} f_{Tt} &= \sum_{i,j=1}^{s} w_i w_j f_{tij} \\ &= 1 - \boldsymbol{W}_t \boldsymbol{D}_t \cdot \ldots \cdot \boldsymbol{D}_{t_1+1}(\boldsymbol{1} - \boldsymbol{f}_{t_1}). \end{aligned} \tag{24}$$

For a Wright–Fisher model of diploid size N, it is easy to see that $1 - f_{Tt}$ drops by $1 - 1/(2N)$ in each generation (see for instance Section 1.7.1 of [30], so that $f_{Tt} = 1 - (1 - f_{Tt_1})(1 - 1/(2N))^{t - t_1}$. Based on this, the inbreeding effective size without replacement over time interval $[t_1, t]$,

$$N_{el}([t_1, t]) = \begin{cases} \dfrac{1}{2\left(1 - \left(\dfrac{\boldsymbol{W}_T \boldsymbol{D}_t \cdots \boldsymbol{D}_{t_1+1}(\boldsymbol{1} - \boldsymbol{f}_{t_1})}{\boldsymbol{W}_T(\boldsymbol{1} - \boldsymbol{f}_{t_1})}\right)^{1/(t-t_1)}\right)}, & \text{if } f_{Tt} > f_{Tt_1}, \\ \mathrm{NaN}, & \text{if } f_{Tt} \le f_{Tt_1}, \end{cases} \tag{25}$$

is defined as the size of a Wright–Fisher population for which $(1 - f_{Tt})/(1 - f_{Tt_1})$ decreases by the same amount as in the studied population.

In the lower part of (25) we incorporated the possibility that the IBD probability f_{Tt} does not increase between generations t_1 and t, so that $N_{el}([t_1, t])$ is not well defined. Since plausible scenarios can be found when this happens, this is a deficiency of N_{el}. For instance, if positive weights are assigned only to a subset $\mathcal{S}$ of subpopulations, as in (14), and the amount of inbreeding $f_{t_1 ij}$ for i, j within $\mathcal{S}$ is much larger than $f_{t_1 ij}$ with $i \in \mathcal{S}$ and $j \notin \mathcal{S}$, then f_{Tt} may decrease the first few generations $t > t_1$ due to migration into $\mathcal{S}$ from the less inbred subpopulations outside $\mathcal{S}$.

Definition (25) has a very appealing property

$$N_{el}([t_1, t]) = \frac{1}{2\left(1 - \prod_{r=t_1}^{t-1}\left(1 - \frac{1}{2N_{el}([r, r+1])}\right)^{1/(t-t_1)}\right)}, \tag{26}$$

whenever each term $N_{el}([r, r+1])$ on the right hand side is well defined according to (25) for each value of the generation index r. In particular, for large populations, $N_{el}([t_1, t])$ is approximately the harmonic mean of all $N_{el}([r, r+1])$, as for homogeneous populations [19, p. 144].

Suppose $\mathcal{S} = \{i\}$ consists of a single subpopulation, with weights $w_j = 1_{\{j=i\}}$ in (14). When there is migration from at least one of the other subpopulations into i, (26) describes how the local effective size of i over $[t_1, t]$ depends on the local effective sizes of i between subsequent generations. These will in general differ from N_{eti}, since they are also affected by immigration into i. It is shown in Appendix A that this confounding effect disappears and

$$N_{el}([t, t+1]) = N_{eti} \tag{27}$$

when i receives no immigrants from the other subpopulations.

The backward interpretation of (25) simplifies when $t_1 = t_0$ is the founder generation. Then $f_{tij} = f^{\mathrm{IBD}}_{t_0 tij}$ is the probability that two distinct genes, drawn from i and j in generation t, have found their most recent common ancestor (MRCA) within time span $t - 1, t - 2, \ldots, t_0$, so that $f_{t_0 ij} = 0$ gives an initial condition $\boldsymbol{f}_{t_0} = \boldsymbol{0}$ in (24). Suppose two distinct genes of generation t are drawn according to sampling scheme T, and let τ_{Tt} be their coalescence time, corresponding to a MRCA from generation $t - \tau_{Tt}$. Then we can rewrite (24) as $f_{Tt} = f_{Tt_0 t} = P(\tau_{Tt} \le t - t_0)$, and (25) simplifies to

$$\begin{aligned} N_{el}([t_0, t]) &= \frac{1}{2\left(1 - (1 - P(\tau_{Tt} \le t - t_0))^{1/(t-t_0)}\right)} \\ &= \frac{1}{2\left(1 - (\boldsymbol{W}_T \boldsymbol{D}_t \cdot \ldots \cdot \boldsymbol{D}_{t_0+1}\boldsymbol{1})^{1/(t-t_0)}\right)}. \end{aligned} \tag{28}$$

In particular, for a time interval $[t, t+1]$, (28) equals

$$N_{el}([t, t+1]) = \frac{1}{2P(\tau_{T,t+1} = 1)} = \frac{1}{2\left(1 - \boldsymbol{W}_T \boldsymbol{D}_{t+1}\boldsymbol{1}\right)},$$

which for an isolated ($s = 1$) population simplifies to $N_{et} = N_{et1}$, in accordance with the original N_{el} definition of [113], see for instance equation 7.6.2.8 of [18] or Section 4.4 of [19].

4.1.2. Drawing with replacement

If we rather draw two genes *with* replacement from subpopulations i and j of generation t, their IBD probability is

$$\mathcal{F}_{tij} = \sum_{c=1}^{2N_{t_0}} \mathcal{P}_{tic}\mathcal{P}_{tjc} \tag{29}$$

for all $1 \le i, j \le s$. The definitions of the expected IBD probabilities $f_{tij} = f_{t_1 tij}$ and f_{Tt} in (23)–(24) remain the same, apart from replacing matrices $\boldsymbol{D}_t$ by $\boldsymbol{A}_t$ everywhere. For a Wright–Fisher population with diploid size N, it holds that $f_{Tt} = 1 - (1 - f_{Tt_1})(1 - 1/(2N))^{(t-t_1)}$, see for instance Theorem 1.3 of [19]. Based on this observation, we define the inbreeding effective size N_{el} (with replacement) over time interval $[t_1, t]$ as

$$N_{el}([t_1, t]) = \begin{cases} \dfrac{1}{2\left(1 - \left(\dfrac{\boldsymbol{W}_T \boldsymbol{A}_t \cdots \boldsymbol{A}_{t_1+1}(\boldsymbol{1} - \boldsymbol{f}_{t_1})}{\boldsymbol{W}_T(\boldsymbol{1} - \boldsymbol{f}_{t_1})}\right)^{1/(t-t_1)}\right)}, & \text{if } f_{Tt} > f_{Tt_1}, \\ \mathrm{NaN}, & \text{if } f_{Tt} \le f_{Tt_1}. \end{cases} \tag{30}$$

4.2. Nucleotide diversity effective size

The mutation or nucleotide diversity effective size $N_{e\pi}$ is the size of a Wright–Fisher population with the same heterozygosity in generation t as in the studied population at a site with a very small mutation probability, see [19,22]. It is defined in terms of the expected coalescence time τ_{Tt} of two genes, sampled in generation t according to scheme T;

$$N_{e\pi}([t-\|\tau_{Tt}\|,t]) = \frac{E(\tau_{Tt})}{2}, \tag{31}$$

with $\|\tau_{Tt}\|$ the smallest positive integer such that $P(\tau_{Tt} \le \|\tau_{Tt}\|) = 1$. In particular, if τ_{Tt} has no finite upper bound, the time interval in (31) equals $(-\infty, t]$. It follows from (24) and (31) that

$$\begin{aligned} N_{e\pi}([t-\|\tau_{Tt}\|,t]) &= \frac{1}{2}\sum_{r=0}^{\|\tau_{Tt}\|-1} P(\tau_{Tt} > r) \\ &= \frac{1}{2}\left(1+\sum_{r=1}^{\|\tau_{Tt}\|-1} \boldsymbol{W}_T\boldsymbol{D}_t\cdot\ldots\cdot\boldsymbol{D}_{t-r+1}\mathbf{1}\right). \end{aligned} \tag{32}$$

4.3. Variance effective size

Consider a biallelic gene ($n_t = 2$), and write the allele frequencies of the two alleles (1 and 2) of subpopulation i in generation t as $P_{ti1} = P_{ti}$ and $P_{ti2} = 1 - P_{ti}$. We will make the simplifying assumption that all subpopulations have the same frequency $P_{01} = \ldots = P_{0s} =: P_0$ of allele 1 in generation $t = 0$. Without this assumption, the variance effective size is much more difficult to analyze ([21,36]). Let $\mathrm{Cov}_0(\cdot,\cdot)$ refer to the covariance between two random variables conditionally on allele frequencies of the $t = 0$ generation. For any pair of subpopulations i and j,

$$f_{tij} = f_{tij}^{\mathrm{cov}} = \frac{\mathrm{Cov}_0(P_{ti}-P_0, P_{tj}-P_0)}{P_0(1-P_0)} \tag{33}$$

quantifies how correlated their genetic drifts over time interval $[0, t]$ are.

It is shown in Appendix A that the column vector $\boldsymbol{f}_t = \boldsymbol{f}_t^{\mathrm{cov}} = (f_{tij})$ satisfies a special case of recursion (8) for genes drawn *with* replacement, with $\mu = 0$ and initial condition $\boldsymbol{f}_t = \mathbf{0}$. Jorde and Ryman [37] obtained analogous recursions for genetic drift variables of age-structured models, where subpopulations represent age classes, whose sizes are constant over time, Felsenstein [26], Tufto et al. [97] and Tufto and Hindar [98] derived covariance recursions for a slightly different reproduction model than ours, and Emigh [20] studied related recursions for variances of allele frequencies.

Let

$$P_t = \sum_{i=1}^{s} w_i P_{ti}$$

be the overall frequency of allele 1 in the total population when subpopulations are weighted as $w_1, \ldots, w_s$. It then follows from (33) and the above mentioned recursions that the genetic drift over time interval $[0, t]$ is

$$\begin{aligned} \frac{\mathrm{Var}_0(P_t-P_0)}{P_0(1-P_0)} &= \sum_{i,j=1}^{s} w_i w_j \frac{\mathrm{Cov}_0(P_{ti},P_{tj})}{P_0(1-P_0)} \\ &= \sum_{i,j=1}^{s} w_i w_j f_{tij} \\ &= f_{Tt} \\ &= 1 - \boldsymbol{W}_T\boldsymbol{A}_t\cdot\ldots\cdot\boldsymbol{A}_1\mathbf{1}. \end{aligned} \tag{34}$$

The variance effective size $N_{eV}([0, t])$ over time interval $[0, t]$ is defined as the number of individuals of a diploid Wright–Fisher model for which f_{Tt} is the same as in (34). Since $f_{Tt} = 1 - (1 - 1/(2N))^t$ for a Wright–Fisher model of diploid size N (see for instance Section 5.1.2 of [65]) this leads to

$$N_{eV}([0,t]) = \frac{1}{2(1-(\boldsymbol{W}_T\boldsymbol{A}_t\cdot\ldots\cdot\boldsymbol{A}_1\mathbf{1})^{1/t})}, \tag{35}$$

a special case of the version (30) of $N_{el}([0, t])$ with genes drawn with replacement, when there is no subpopulation differentiation at $t = 0$, i.e. $f_{0ij} = f_0$ for all i, j and some $0 < f_0 < 1$. In particular, for a time interval $[0, 1]$ of one single generation *ahead* of the present, (35) simplifies to

$$N_{eV}([0,1]) = \frac{P_0(1-P_0)}{2\mathrm{Var}_0(P_1-P_0)} = \frac{1}{2(1-\boldsymbol{W}_T\boldsymbol{A}_1\mathbf{1})}. \tag{36}$$

For an homogeneous ($s = 1$) population the first part of (36) agrees with [16], and in particular we find that $N_{eV}([0, 1]) = N_{11}$ if $N_{0e1} = N_{01}$.

4.4. Eigenvalue effective size

The eigenvalue effective size N_{eE} [16,21,23] is defined as the number of individuals of a diploid Wright–Fisher model for which the multiplicative rate λ at which alleles are lost is the same as in the studied population. It has been shown [35,110] that λ also equals the rate at which predicted gene identities approach 1. In other words, N_{eE} defines the rate at which inbreeding increases at equilibrium in all subpopulations.

A Wright–Fisher model of diploid size N has $\lambda_{\mathrm{WF}} = 1 - 1/(2N)$, see for instance [24]. Equating λ with λ_{WF} and solving for N, we find that

$$N_{eE} = N_{eE}([t_1,\infty)) = \frac{1}{2(1-\lambda)} \tag{37}$$

for any $t_1 \ge t_0$. In Section 5.4 we prove that N_{eE} is the same whether genes are drawn with or without replacement. We may therefore assume that $\boldsymbol{f}_t$ is the vector of predicted gene identities with genes drawn with replacement. Existence of λ requires some extra condition, such as a population size that varies according to a Markov chain [39] or cyclically [77,79,104,105]. If all population characteristics vary cyclically with period $\tau > 0$, it follows that $\boldsymbol{A}_{t+\tau} = \boldsymbol{A}_t$ for all $t \ge 1$, so that

$$\boldsymbol{f}_{t_1+n\tau+r} = \mathbf{1} - \boldsymbol{A}_{r+t_1}\cdot\ldots\cdot\boldsymbol{A}_{1+t_1}\cdot(\boldsymbol{A}_\tau\cdot\ldots\cdot\boldsymbol{A}_1)^n(\mathbf{1}-\boldsymbol{f}_{t_1}), \tag{38}$$

for any $n \ge 0$ and $0 \le r \le \tau - 1$. Under mild conditions, $\boldsymbol{A}_{1:\tau} = \boldsymbol{A}_\tau \cdot \ldots \cdot \boldsymbol{A}_1$ is irreducible and aperiodic, and then it follows from Perron–Frobenius Theorem (see for instance [15]) that a unique largest and positive eigenvalue $\lambda_{\max}(\boldsymbol{A}_{1:\tau})$ of $\boldsymbol{A}_{1:\tau}$ exists, which will determine the rate

$$\lambda = \lambda_{\max}(\boldsymbol{A}_\tau\cdot\ldots\cdot\boldsymbol{A}_1)^{1/\tau} \tag{39}$$

of increase of the expected gene identities (38). Inserting (39) into (37), we find that N_{eE} is the only effective size independent of the weighting scheme $\boldsymbol{w}$. It is a global effective size, even if $w_i = 0$ for some subpopulations i.

5. Constant subpopulation sizes and migration rates

Suppose all subpopulation sizes $N_{ti} = N_i$, forward migration rates $M_{tki} = M_{ki}$ and local effective sizes $N_{eti} = N_{ei}$ are constant over time. Write the total subpopulation size as $N = \sum_{i=1}^{s} N_{ti}$, the matrix of forward migration rates as $\boldsymbol{M} = (M_{ki})$ and introduce the vector $\boldsymbol{u} = (u_1, \ldots, u_s)$ of relative subpopulation sizes $u_i = N_i/N$. It follows from (1) that $\boldsymbol{u}$ is a left eigenvector of $\boldsymbol{M}$ with eigenvalue 1, corresponding to a system

$$\begin{aligned} \boldsymbol{u} &= \boldsymbol{u}\boldsymbol{M}, \\ \textstyle\sum_{i=1}^{s} u_i &= 1, \end{aligned} \tag{40}$$

of $s+1$ equations, from which all u_i can be inferred, given a specification of $\boldsymbol{M}$. In view of (2), the backward migration rates $B_{tik} = B_{ik}$ are constant over time as well, and related to the forward migration rates as

$$B_{ik} = \frac{u_k M_{ki}}{u_i}. \tag{41}$$

Since $\sum_k B_{ik} = 1$ for any i, $\boldsymbol{B} = (B_{ik})$ is the transition matrix of a Markov chain with s states. We assume that this Markov chain is irreducible and aperiodic, with a unique equilibrium distribution

$$\boldsymbol{\gamma} = (\gamma_1, \ldots, \gamma_s). \tag{42}$$

Intuitively, γ_i is the probability that a distant ancestor of a gene that is sampled from any subpopulation of the present, has its ancestor a large number of generations back in time from subpopulation i.

5.1. Subpopulation weights

When local census sizes are constant over time, it is of interest to weight the subpopulations $\mathcal{S}$ from which we collect data proportionally to size, i.e.

$$w_i = \frac{u_i 1_{\{i\in\mathcal{S}\}}}{\sum_{j\in\mathcal{S}} u_j}. \tag{43}$$

This implies that all genes that belong to $\mathcal{S}$ have the same sampling probability, whereas those outside $\mathcal{S}$ will not be sampled. In particular

$$w_i = u_i \tag{44}$$

corresponds to a scenario where all genes in the population are drawn with the same probability. Another possibility is to use as weights the probabilities

$$w_i = \gamma_i \tag{45}$$

in (42), see [25,36,61,108]. We will refer to (45) as reproductive weights, since each subpopulation is weighted proportionally to its *long term* number of offspring. For this reason, they are useful when long term genetic changes of the population are to be inferred from short term changes.

5.2. Gene identities, gene diversities and subpopulation differentiation

When genes are drawn with replacement, the recursions in (8) for the predicted gene identities and gene diversities simplify to

$$\begin{aligned} \boldsymbol{f}_t &= (1-\mu)^2(\boldsymbol{A}\boldsymbol{f}_{t-1} - \boldsymbol{A}\boldsymbol{1} + \boldsymbol{1}) + \left(1-(1-\mu)^2\right)\boldsymbol{\delta}, \\ \boldsymbol{h}_t &= (1-\mu)^2\boldsymbol{A}\boldsymbol{h}_{t-1} + \left(1-(1-\mu)^2\right)(\boldsymbol{1}-\boldsymbol{\delta}), \end{aligned} \tag{46}$$

for $t = 1, 2, 3, \ldots$, where $\boldsymbol{A} = (A_{ij,kl})$ has elements

$$A_{ij,kl} = \left(1 - \frac{1}{2Nu_i}\right)^{\{i=j\}} B_{ik}B_{jl}\left(\frac{1-\frac{1}{2N_{ek}}}{1-\frac{1}{2Nu_k}}\right)^{\{k=l\}}, \tag{47}$$

and $\boldsymbol{\delta} = (\delta_{ij})$ is a column vector of length s^2, with entries $\delta_{ij} = 1_{\{i=j\}}/(2Nu_i)$. Analogously, when genes are drawn without replacement, the recursions in (11) for the predicted gene identities and gene diversities, simplify to

$$\begin{aligned} \boldsymbol{f}_t &= (1-\mu)^2(\boldsymbol{D}\boldsymbol{f}_{t-1} - \boldsymbol{D}\boldsymbol{1} + \boldsymbol{1}), \\ \boldsymbol{h}_t &= (1-\mu)^2\boldsymbol{D}\boldsymbol{h}_{t-1} + \left(1-(1-\mu)^2\right)\boldsymbol{1}, \end{aligned} \tag{48}$$

for $t = 1, 2, 3, \ldots$, where $\boldsymbol{D} = (D_{ij,kl})$ has elements

$$D_{ij,kl} = B_{ik}B_{jl}\left(1 - \frac{1}{2N_{ek}}\right)^{\{k=l\}}, \tag{49}$$

and (48) agrees with a classical recursion in [56]. Gene identity recursions have been studied in other settings by Caballero [8] and Nagylaki [62] for dioecious (two-sex) models, in which sexes correspond to subpopulations, and Sawyer [86] for the diploid stepping stone model.

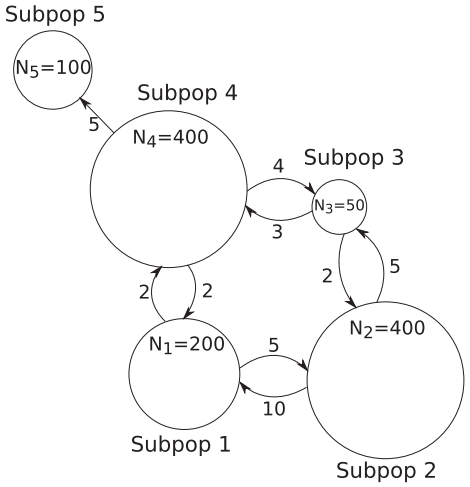

Fig. 1. Population system with five subpopulations and local census sizes $N_i = N_{ti} = N_{eti}$ that are constant over time. The arrows illustrate migration between different pairs k, i of subpopulations, and next to them the number of migrants $N_k M_{ki}$ from k to i per generation, so that for instance $M_{11} = 0.94$, $M_{12} = 0.025$, $M_{14} = 0.01$ and $M_{13} = M_{15} = 0$.

When genes are drawn with replacement and mutations are absent ($\mu = 0$), (20) and (46) imply that the predicted coefficient of gene differentiation over time interval $[0, t]$ simplifies to

$$g_{STt}([0,t]) = \frac{(\boldsymbol{W}_T - \boldsymbol{W}_S)\boldsymbol{A}^t(\boldsymbol{1}-\boldsymbol{f}_0)}{\boldsymbol{W}_T\boldsymbol{A}^t(\boldsymbol{1}-\boldsymbol{f}_0)}, \tag{50}$$

and asymptotically for large time intervals, we find from a Jordan decomposition of $\boldsymbol{A}$ (see for instance [15]) that

$$g_{ST\infty} = \lim_{t\to\infty} g_{STt}([0,t]) = \frac{(\boldsymbol{W}_T - \boldsymbol{W}_S)\boldsymbol{r}}{\boldsymbol{W}_T\boldsymbol{r}}, \tag{51}$$

with $\boldsymbol{r}$ the right eigenvector of the largest eigenvalue of $\boldsymbol{A}$. Eq. (51) is related to a quasi equilibrium approximation of $G_{ST,t}$ in [36], and an asymptotic expression of the fixation index in [82], in terms of ratios of tail probabilities of coalescence times of genes from different pairs of subpopulations. The convergence rate in (51) is exponentially fast $O\left((\lambda_2/\lambda_1)^t\right)$, with $\lambda_1 = \lambda_{\max}(\boldsymbol{A}) > \lambda_2$ the two largest eigenvalues of $\boldsymbol{A}$.

Example 1 (**A system with five subpopulations).** Consider the population of Fig. 1. It has no novel mutations ($\mu = 0$) and consists of five subpopulations $i = 1, \ldots, 5$ whose local census and effective sizes are the same and constant over time ($N_{ti} = N_{eti} = N_i$). The migration matrix $\boldsymbol{M} = (M_{ki})$ is also constant over time, with four subpopulations connected through migration along a circle, whereas the fifth subpopulation has no emigrants. It is only linked with the other subpopulations through immigration from subpopulation 4.

Fig. 2 shows predictions of gene identities (with replacement) for each subpopulation i separately (f_{tii}), for subpopulations combined (f_{St}) and for the total population (f_{Tt}). As expected, they all tend to 1 as the length of the prediction interval (t) increases. The amount of inbreeding f_{0ij} at $t = 0$ varies within and between subpopulations, and although initially subpopulation 5 has the least amount of inbreeding, it soon becomes most inbred. It is seen that the values of f_{0ij} when $i \neq j$ have a great impact on the overall level of future inbreeding.

If subpopulation number i would have been isolated, then

$$f_{tii} = 1 - (1-f_{0ii})(1-1/(2N_i))^t, \tag{52}$$

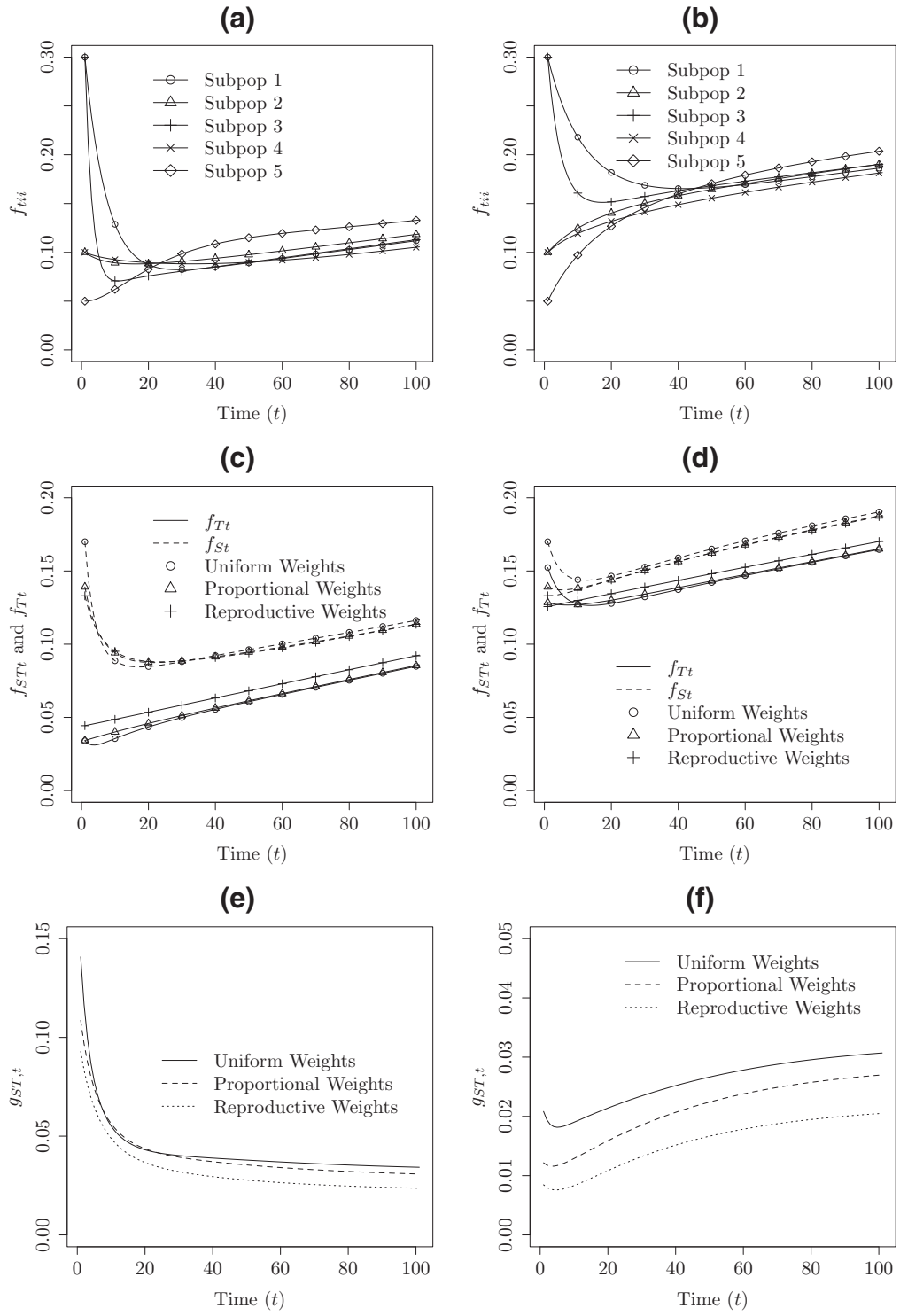

Fig. 2. Amount of inbreeding and subpopulation differentiation, as a function of generation (t) for all subpopulations $i = 1, \ldots, 5$ of Fig. 1 in absence of mutations ($\mu = 0$). The columns differ in whether the amount of inbreeding between subpopulations in generation 0 is minimal, left, or maximal, right (see below). The plots show a, b) predicted gene identities f_{tii} with replacement (5), c, d) the corresponding predicted gene identities f_{Tt} and f_{St} in (19), for the total population and within subpopulations, weighted uniformly (15), proportionally to size (44) or reproductively (45), e, f) predicted coefficients of gene differentiation g_{STt} in (18), for all three weighting schemes. The gene identities of generation 0 within the subpopulations are $f_{011} = 0.3, f_{022} = 0.1, f_{033} = 0.3, f_{044} = 0.1$ and $f_{055} = 0.05$, and between subpopulations $f_{0ij} = 0$ (left), $f_{0ij} = \sqrt{f_{0ii} f_{0jj}}$ (right), corresponding to the lower and upper limits of (6). Note the different scales on the vertical axes.

which is very different from the true curves, shown in the upper two subplots. Subpopulations 1 and 3 both have a large proportion of immigrants, and the first few generations their levels of inbreeding decrease, in contrast to (52). For all five subpopulations, the long term multiplicative rate of increased inbreeding is $1 - 1/(2N_{eE}) = 0.9995$ per generation (see Example 3), much less than predicted by (52). This highlights the importance of avoiding isolation, particularly for small subpopulations.

The predicted coefficient of gene differentiation (g_{STt}) is shown for all three weighting schemes, and it converges to nonzero limits

as t increases. Since the ratio of the two largest eigenvalues of $\boldsymbol{A}$ is $\lambda_2/\lambda_1 = 0.988$, it follows from the paragraph below (51) that although the convergence rate towards $g_{ST\infty}$ is exponential $O(0.988^t)$, it is still very slow, and therefore the whole time profile of g_{STt} is needed. The reproductive weights give the smallest and the uniform weights the largest values of $g_{ST\infty}$, with the size-proportional weights in between.

5.3. Coalescence probabilities and expected coalescence times

We noticed in Section 4.1 that coalescence probabilities f_{t_0tij} satisfy the same forward recursion as gene identities in absence of mutations, when the founder generation t_0 is kept fixed and t increases. Slatkin [90] and Nagylaki [63] obtained an analogous backward recursion

$$\boldsymbol{h}_{t_0,t} = \boldsymbol{D}\boldsymbol{h}_{t_0+1,t} \quad t_0 = t-1, \quad t-2, \ldots \tag{53}$$

for the non-coalescence probabilities $\boldsymbol{h}_{t_0t} = \boldsymbol{1} - \boldsymbol{f}_{t_0t}$ when subpopulation sizes are constant. We may in fact interpret (53) as the transition probabilities of a structured coalescent [33,72] in discrete time for a sample of two lineages.

Slatkin [90] used recursion (53) to derive an explicit expression for the expected coalescence time of two genes sampled from an island model of constant size. This approach can be extended to our general framework of migration, reproduction and subpopulation weights w_i. Then τ_{Tt} is the coalescence time of two genes sampled in generation t with scheme T, and

$$\begin{aligned} E(\tau_{Tt}) &= \sum_{r=0}^{\infty} P(\tau_{Tt} > r) \\ &= \sum_{r=0}^{\infty} \boldsymbol{W}_T \boldsymbol{D}^r \boldsymbol{1} \\ &= \boldsymbol{W}_T (\boldsymbol{I} - \boldsymbol{D})^{-1} \boldsymbol{1}. \end{aligned} \tag{54}$$

It follows from (54) that τ_{Tt} has a discrete phase-type distribution [5,71], i.e. the time until absorption of a Markov chain describing the joint subpopulation ancestry of two different genes. Its state space of size s^2+1 contains all s^2 ordered pairs of subpopulations (before the genes have coalesced), and an additional absorbing state after coalescence. It starts with initial distribution $\boldsymbol{W}_T$ among the non-absorbing states, and $\boldsymbol{D}$ contains the transition probabilities between all non-absorbing states.

In view of (31), formula (54) provides an explicit expression

$$N_{e\pi} = N_{e\pi}((-\infty, t]) = \frac{1}{2}\boldsymbol{W}_T (\boldsymbol{I} - \boldsymbol{D})^{-1} \boldsymbol{1} \tag{55}$$

for the nucleotide diversity effective size, with $\boldsymbol{I}$ the identity matrix of order s^2. Strobeck [94] and Durrett [19, p. 149] have studied models for which $\boldsymbol{B}$ is doubly stochastic, so that not only the column sums, but also the row sums, equal 1. Then all subpopulations are equally large and reproductive ($u_i = \gamma_i = 1 = 1/s$), and for a local weighting scheme $w_j = 1_{\{j=i\}}$ of any subpopulation i, they prove that $N_{e\pi} = N$, provided that $N_{ej} = Nu_j$ for all subpopulations j. On the other hand, $N_{e\pi}$ will be larger than N for any scheme $\boldsymbol{w}$ that assigns positive weights to at least two subpopulations.

We may also introduce the coalescence time τ_{St} of two genes sampled in generation t according to scheme S, and a prediction

$$g_{STt}((-\infty, t]) = \frac{E(\tau_{Tt}) - E(\tau_{St})}{E(\tau_{Tt})} = \frac{(\boldsymbol{W}_T - \boldsymbol{W}_S)(\boldsymbol{I} - \boldsymbol{D})^{-1}\boldsymbol{1}}{\boldsymbol{W}_T(\boldsymbol{I} - \boldsymbol{D})^{-1}\boldsymbol{1}} \tag{56}$$

of the coefficient of gene differentiation in generation t, in the limit of small mutation rates $\mu \to 0$. Formula (56) generalizes a suggestion of Slatkin [90] for the island model. It is similar to (50), but has another definition of predicted gene diversity, in terms of the probability that mutation comes before coalescence when looking backwards in time. For this reason, we write the interval in (56) as $(-\infty, t]$. It is shown in [36] that (56) is asymptotically equivalent to a version of (50)–(51) with $\boldsymbol{D}$ in place of $\boldsymbol{A}$, in the limit of large population sizes. Wilkinson-Herbots [112] obtained extensions of (56) for non-negligible mutation rates μ.

5.4. Eigenvalue effective size

In absence of mutations, the upper part of (46) gives an explicit formula $\boldsymbol{f}_t = \boldsymbol{1} - \boldsymbol{A}^t(\boldsymbol{1} - \boldsymbol{f}_0)$ for the predicted gene identity, first obtained in [25] for age-structured models. Since the backward matrix $\boldsymbol{B}$ is irreducible and aperiodic, it follows that $\boldsymbol{A}$ is irreducible and aperiodic as well. We can use Perron Frobenius' Theorem and conclude that $\boldsymbol{A}$ has a unique positive largest eigenvalue $\lambda_{\max}(\boldsymbol{A})$, which determines the long term multiplicative rate of increase of predicted gene identities, with an eigenvalue effective size

$$N_{eE} = N_{eE}([0, \infty)) = \frac{1}{2(1 - \lambda_{\max}(\boldsymbol{A}))}, \tag{57}$$

that is a special case of (37) and (39), corresponding to a cycle of length $\tau = 1$, see [35,98,110]. In Appendix A we show that $\boldsymbol{A}$ can be replaced by $\boldsymbol{D}$ in (57), since

$$\lambda_{\max}(\boldsymbol{A}) = \lambda_{\max}(\boldsymbol{D}), \tag{58}$$

and moreover, the whole spectrum of eigenvalues is the same for $\boldsymbol{A}$ and $\boldsymbol{D}$, at least when all eigenvalues are distinct. As mentioned in Section 4.4, the conclusion is that N_{eE} is the same, regardless of whether we use a version of predicted gene diversities with genes drawn with or without replacement.

Example 2 (**The effect of varying the migration rate on** N_{eE})**.** Consider again the population of Fig. 1. In Fig. 3 we have plotted the eigenvalue effective size N_{eE} in (57) and the predicted coefficient of gene differentiation $g_{ST\infty}$ in (51) as a function of the overall migration rate

$$m = 1 - \sum_{i=1}^{s} u_i M_{ii}, \tag{59}$$

i.e. the fraction of genes whose offspring live in another subpopulation than their parents. In order to vary $\boldsymbol{M}$ (and hence also m) we reduced the migration rates of Fig. 1 by multiplying the numbers at the arrows with a variable factor $0 < a \leq 1$. For each value of a we increased the number of offspring that remain at their parental subpopulations accordingly.

We notice that $N_{eE} \to \infty$ and $g_{ST\infty} \to 1$ as $m \to 0$, and from the lower left subplot

$$N_{eE} = \frac{CN}{1 - g_{ST\infty}} + o\left(\frac{1}{1 - g_{ST\infty}}\right), \tag{60}$$

with $C = 0.793$.

Both $N_{e\pi}$ and N_{eE} in (55) and (57) quantify the long term behavior of the population. In general they differ, since $N_{e\pi}$ depends on the weighting scheme $\boldsymbol{w}$ whereas N_{eE} does not. They are only asymptotically equivalent in the limit of large population sizes, see [36].

5.5. Time dynamics of inbreeding and variance effective size

The (different versions of the) inbreeding and variance effective sizes are defined for time intervals of finite length. It follows from (28), (30), (35), (57) and (58) that they are all asymptotically equivalent to the eigenvalue effective size over large time intervals, since

$$\lim_{t\to\infty} N_{el}([0, t]) = \lim_{t\to\infty} N_{eV}([0, t]) = N_{eE}, \tag{61}$$

regardless of weights $\boldsymbol{w}$, see Appendix A for details. A bit surprisingly, the convergence rate $O(1/t)$ in (61) is slow, regardless of the spectrum of eigenvalues of $\boldsymbol{A}$ and $\boldsymbol{D}$. However, if genes are drawn with replacement and either $\boldsymbol{W}_T = \boldsymbol{\rho}$ or $\boldsymbol{h}_0 = \boldsymbol{r}$, where $\boldsymbol{\rho}$ and $\boldsymbol{r}$ are the left

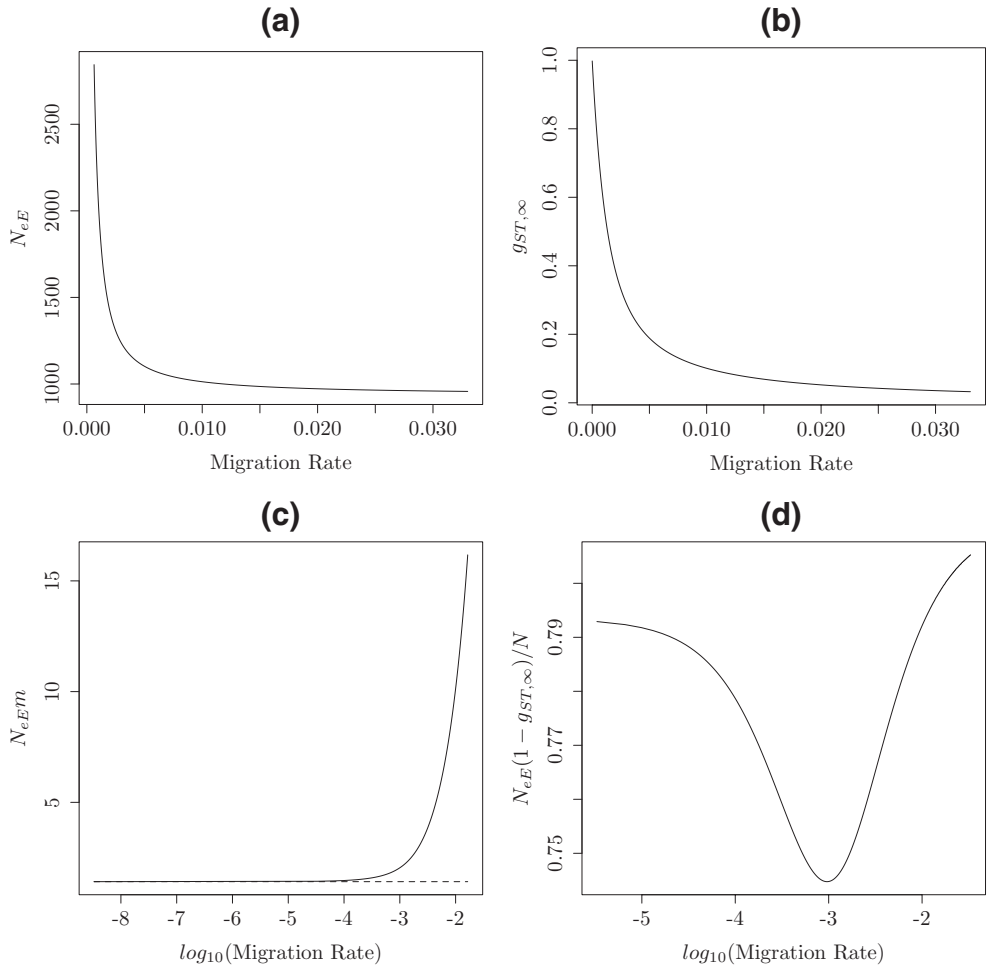

Fig. 3. Plot of the eigenvalue effective size N_{eE} (a), long term predicted coefficient of gene differentiation $g_{ST\infty}$ (b), $N_{eE}m$ (c) and $N_{eE}(1-g_{ST\infty})/N$ (d), as a function of the migration rate m in (59), for a system with five subpopulations and census sizes as in Fig. 1. The mutation rate $\mu = 0$ and the migration rate from subpopulation k to $i \neq k$ is $M_{ki} = M_{ki}(a) = aM_{ki}(1)$, where $0 < a \leq 1$ and $M_{ki}(1)$ is the corresponding migration rate in Fig. 1. The diagonal elements M_{ii} of the migration matrix are defined to ensure that all local census sizes remain constant over time. The lower left subplot converges to 1.419 as $m \to 0$, and the lower right subplot to $C = 0.793$ as $m \to 0$, in accordance with (60).

and right eigenvectors corresponding to the largest eigenvalue of $\boldsymbol{A}$, then $N_{eI}([0,t]) = N_{eE}$ for any $t = 1, 2, \ldots$. The same is true if genes are drawn without replacement, if either $\boldsymbol{W}_T = \tilde{\boldsymbol{\rho}}$ or $\boldsymbol{h}_0 = \tilde{\boldsymbol{r}}$, where $\tilde{\boldsymbol{\rho}}$ and $\tilde{\boldsymbol{r}}$ are the left and right eigenvectors corresponding to the (same) largest eigenvalue of $\boldsymbol{D}$.

Example 3 (**Time dynamics of global** N_{eI})**.** In the first three subplots a–c) of Fig. 4, we study the global inbreeding effective size $N_{eI}([0,t])$ for the population system of Fig. 1, plotted as a function of the number of generations (t) of genetic change, when a number of factors are varied. It is seen that the sampling mechanism, without (25) or with (30) replacement, and the (small) amount of initial fluctuations of the IBD probabilities f_{0ij} at time $t = 0$, both have minor effects on N_{eI}. This is particularly true when the same sampling mechanism is used to define f_{0ij} and N_{eI}. The variance effective size N_{eV} curves are not shown, but they will be close to the N_{eI} curves with replacement, and in the upper left subplot they are identical, since there is no subpopulation differentiation at $t = 0$.

The N_{eI} curves depend a lot on whether uniform (15), size-proportional (44) or reproductive (45) subpopulation weights are used. As t increases, the N_{eI} curves will eventually approach the eigenvalue effective size N_{eE}, as shown in (61), although the convergence rate $O(1/t)$ is slow for the uniform and size-proportional weights. It is only the reproductive weights that give a rapid convergence, since the weight vector $\boldsymbol{W}_T = (\gamma_i\gamma_j;\ 1 \leq i, j \leq s)$ is then very close to the leading left eigenvectors $\boldsymbol{\rho}$ of $\boldsymbol{A}$ and $\tilde{\boldsymbol{\rho}}$ of $\boldsymbol{D}$ respectively, for draws with and without replacement. It follows from the proof of (57) that this makes both versions of $N_{eI}([0,t])$ very close to N_{eE} for any $t > 0$.

If subpopulation structure was ignored, all N_{eI} curves in (a)–(c) would have a constant value equal to the global census size 1150. This is obviously misleading for uniform and reproductive weights, whereas the N_{eI} curves for size proportional weights will at least start at values close to 1150, so that subpopulation structure can be ignored over short time spans. For longer time intervals, all N_{eI} curves will approach the N_{eE} limit of 970, which is considerably smaller than 1150. This discrepancy can be explained by a number of migrants per generation that is fairly large, and a migration pattern that is not conservative, with individuals in some subpopulations more reproductive than in the others, see [35,61].

To summarize the last two paragraphs for size proportional weights: We can neither replace N_{eI} by its long term limit N_{eE} (since convergence is very slow), nor ignore subpopulation structure and replace N_{eI} by the global census size (since N_{eI} will drift away from this value). We rather need the whole time profile for N_{eI}.

In the lower right subplot we vary the migration rates and sizes of all subpopulations proportionally with time. The global census size is

$$N_t = 1150 \cdot \prod_{r=0}^{t-1} 1.001^{49-r} = 1150 \cdot 1.001^{t(99-t)/2},$$

in generation t, so that subpopulation sizes initially increase up to $t = 49$, reach a maximum $N_{49} = N_{50}$ slightly above 3900, then start to

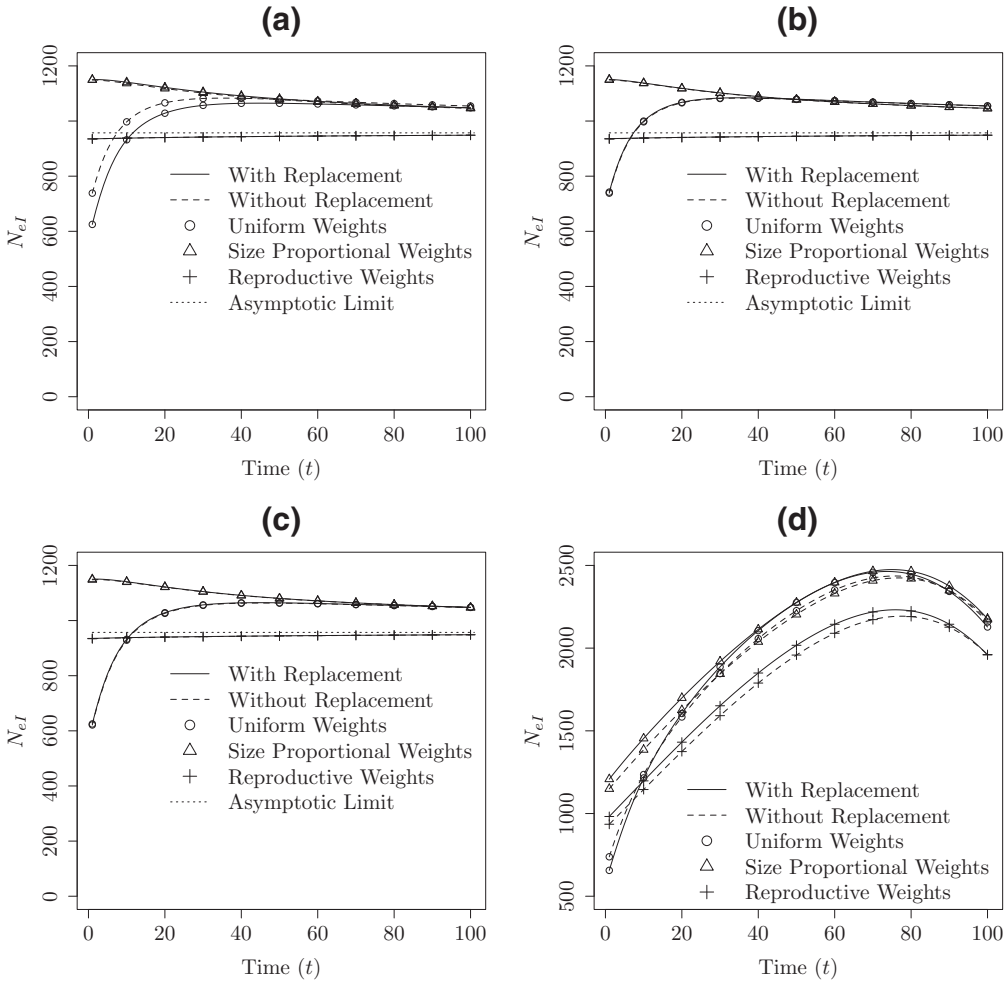

Fig. 4. Global inbreeding effective size $N_{eI}([0,t])$ as a function of the number of generations (t), for the population of Fig. 1 in absence of mutations ($\mu = 0$), using either uniform (15), size-proportional (44) or reproductive (45) subpopulation weights, and sampling without ((25), dashed) or with ((30), solid) replacement. Also shown is the eigenvalue effective size N_{eE} (horizontal dotted). The IBD probabilities f_{0ij} of generation 0 a) are the same for all i, j when genes are drawn with our without replacement, b) all $2\sum_i N_{0i}$ genes of generation 0 are different by descent, with f_{0ij} computed from IBD class frequencies for two genes sampled without (22) or with (29) replacement, c) same as b), but with two IBD classes of equal frequencies 0.5 in all subpopulations, d) same as in a), but the forward migration matrix $\boldsymbol{M}$ of Fig. 1 is replaced by the time varying $\boldsymbol{M}_t = 1.001^{49-t}\boldsymbol{M}$. In a) and d), the global variance effective size $N_{eV}([0,t])$ in (35) coincides with the solid $N_{eI}([0,t])$ curves based on with replacement sampling.

decrease from $t = 52$ until they reach the original $t = 0$ size of Fig. 1 by $t = 99$. The varying population size makes the sampling mechanism more important, since N_{eI} curves with genes drawn without replacement slightly lag those where genes are drawn with replacement. Mathematically we explain this by comparing the local census sizes of the $\boldsymbol{A}_t$ matrices with those of the $\boldsymbol{D}_t$ matrices, which are one time step behind, cf. (85).

In the previous example, we noted that $N_{eI}([0,t])$ converges slowly towards N_{eE}. In contrast $N_{eI}([t,t+\tau])$ will converge exponentially fast at rate $O((\lambda_2/\lambda_1)^t)$ towards N_{eE} as $t \to \infty$, for any fixed $\tau > 0$, since the predicted gene diversities of the left end point t converge exponentially fast to the leading right eigenvector of $\boldsymbol{A}$ or $\boldsymbol{D}$, depending on which sampling scheme that is used.

In the next two examples we demonstrate how subpopulation weights are used to model time dynamics of local and nested inbreeding effective size:

Example 4 (**Time dynamics of local** N_{eI})**.** Fig. 5 displays the local inbreeding effective size $N_{eI}([0,t])$ without replacement (25), for each of the five subpopulations i of Fig. 1, using weights $w_j = 1_{\{j=i\}}$. The subplots differ in whether subpopulation 1 encounters a local bottleneck, or gets temporarily disconnected from subpopulation 2. The local effective sizes of all subpopulations start at values close to their local census sizes, as explained by (27) and the fact that subpopulations exchange very few genes (and hence can be approximately be treated as isolated) during short periods of time. Then they gradually increase towards the eigenvalue effective size N_{eE}. The local bottleneck and interrupted migration temporarily slow down this convergence for subpopulation 1 and (to some extent) its closest neighbors. All five local effective size curves demonstrate that we can neither treat the subpopulations as isolated, since their N_{eI} curves will converge to N_{eE}, nor replace these curves by their limits, since convergence is very slow. We rather need the whole N_{eI} time profile for each subpopulation.

Also shown is the global N_{eI} curve. Since uniform weights (15) are used, the impact of the smaller subpopulations is initially large, with a curve starting at a value less than 2/3 of its asymptotic N_{eE} limit.

Example 5 (**Time dynamics of nested** N_{eI})**.** Fig. 6 plots inbreeding effective size curves $N_{eI}([0,t])$ without replacement (25), as a function of the time t of genetic drift, for nested groups $\mathcal{S} = \{1,\dots,i\}$ of subpopulations ($i = 1,\dots,5$), using either equal or size-proportional weights. The starting values of all curves depend on the local census sizes of the subpopulations in the group and the weighting scheme, and then gradually converge to their asymptotic limits N_{eE}.

If each group $\mathcal{S}$ of subpopulations was a homogeneous and isolated system, its N_{eI} curve would be horizontal, with a constant value equal

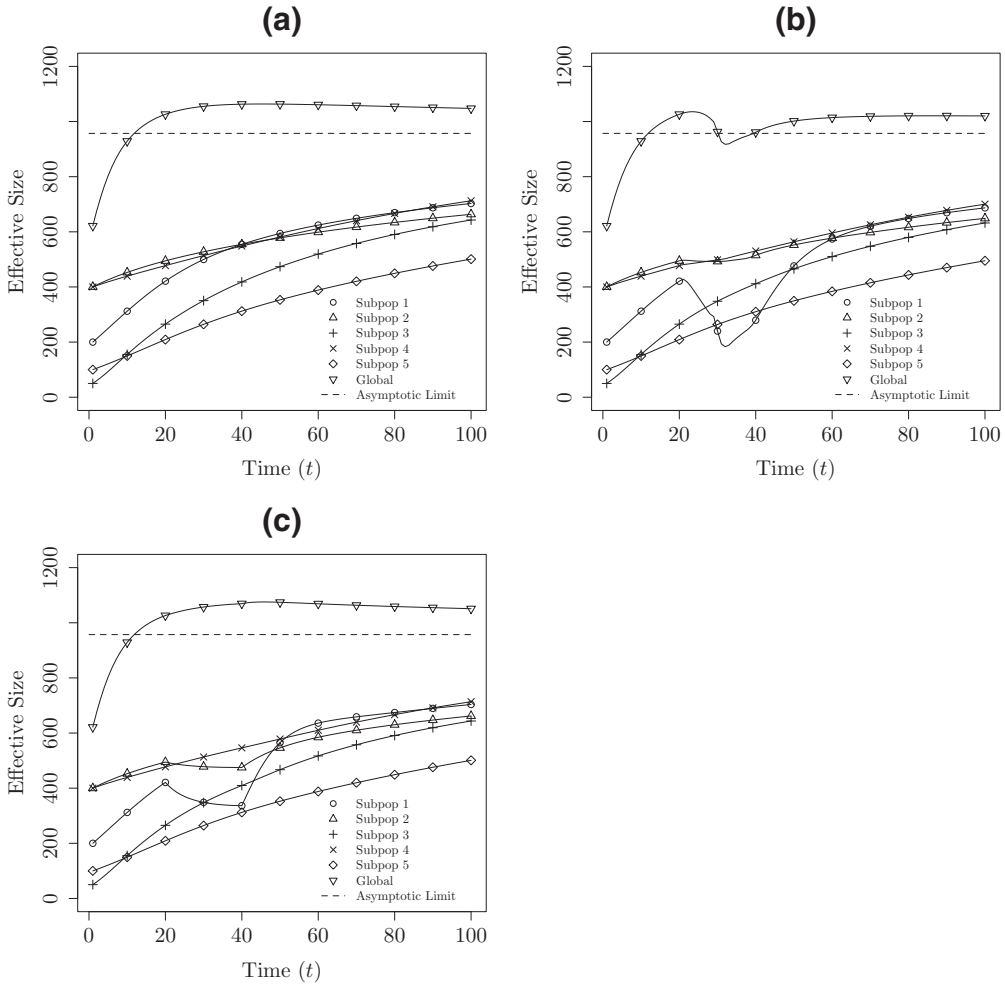

Fig. 5. Local inbreeding effective sizes $N_{el}([0,t])$ with genes drawn without replacement (25), as a function of the number of generations (t) of the time interval of genetic drift, in absence of mutations ($\mu = 0$). There is no subpopulation differentiation in generation 0, with f_{0ij} obtained from (22), (23), and two IBD classes with frequency 0.5 in all subpopulations. Curves are shown for the five subpopulations i, using weights $w_j = 1_{\{j=i\}}$, and for the global inbreeding effective size $N_{el}([0,t])$ with uniform subpopulation weights (15). a) The population equals that of Fig. 1, or the population differs from Fig. 1 in that b) subpopulation 1 encounters a local bottleneck during $t = 21,\ldots,40$, with $N_{t1} = 200, 180, \ldots, 40, 20, 20, 40, \ldots, 180, 200$, c) migration between subpopulations 1 and 2 temporarily drops to 0 during $t = 21,\ldots,40$, and in order to keep the local census sizes of 1 and 2 fixed, both subpopulations are filled up with more parental genes from themselves. The eigenvalue effective size N_{eE} is shown as a horizontal line in all subplots.

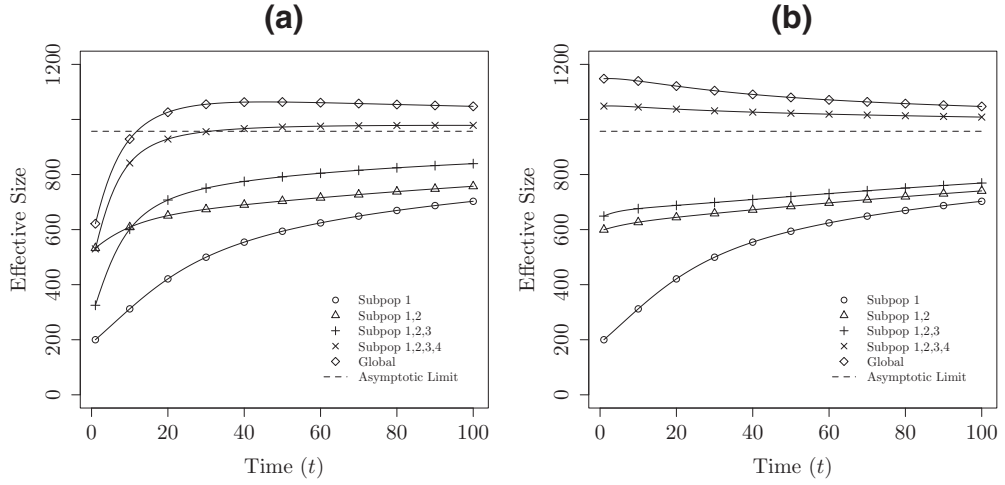

Fig. 6. Inbreeding effective sizes N_{el} ($[0,t]$) as a function of the number of generations (t) of the time interval of genetic drift, for the population of Fig. 1, in absence of mutations ($\mu = 0$), when genes are drawn without replacement (25). There are two IBD classes of the same frequency 0.5 in all subpopulations in generation 0, with f_{0ij} obtained from (22) and (23). Only subpopulations within the groups $\mathcal{S} = \{1,\ldots,i\}$ of subpopulations are assigned positive weights for $i = 1,\ldots,5$, and $i = 5$ gives the global inbreeding effective size. The subpopulations within each group are weighted a) equally (14), b) proportionally to size (43). The horizontal line is the eigenvalue effective size N_{eE} of the whole system.

to the census size $N_1 + \cdots + N_i$ of the group. The corresponding true N_{el} curve in Fig. 6 starts at this value for size proportional weights, but then converges to N_{eE}, since the system is neither isolated (if $i < 5$) nor homogeneous. We rather need the whole N_{el} curve for each group of subpopulations in order to describe its effective size accurately.

6. State space reduction

The predicted gene identity and diversity vectors $\boldsymbol{f}_t$ and $\boldsymbol{h}_t$ include s^2 elements, and their recursions (8) and (11) require $O(s^4)$ operations for each time step. The same is true for the analogous vectors (23) and (33) of IBD probabilities and genetic drift variables. When the number of subpopulations s is large, this is very time consuming, and hence it is of interest to exploit symmetries in order to reduce the state space. For models with translationally invariant migration and reproduction, Fourier analysis can be used to reduce the size of the state space from s^2 to s, see [34] for details. In this section we consider a larger class of models for which the state space can be reduced. For simplicity, we will only deal with the gene identity and gene diversity variables, although analogous results hold for IBD probabilities and genetic drift variables.

We first give general conditions for state space reduction, and then illustrate it with several examples. In more detail, we assume that the collection of all s^2 pairs of subpopulations can be written as a disjoint union

$$\{1,\dots,s\}\times\{1,\dots,s\} = \mathcal{I}_1 \cup \ldots \cup \mathcal{I}_d$$

of d sets. Each of the first d_0 sets consists of equivalent pairs of identical subpopulations, and each of the last $d_1 = d - d_0$ sets consists of equivalent pairs of different subpopulations. More formally, we express this as

$$\mathcal{I}_a \subset \begin{cases} \{(1,1),\dots,(s,s)\}, & 1 \le a \le d_0, \\ \{(i,j),\ 1 \le i \ne j \le s\}, & d_0+1 \le a \le d, \end{cases}$$

require that the local census and effective sizes

$$\begin{aligned} N_{ti} &= \bar{N}_{ta}, \\ N_{eti} &= \bar{N}_{eta}, \end{aligned} \tag{62}$$

are the same for all i such that $(i,i) \in \mathcal{I}_a$ and $a \le d_0$, that the gene identities are constant over each group of pairs of subpopulations when $t = 0$, i.e.

$$F_{0ij} = f_{0ij} = \bar{f}_{0a} \tag{63}$$

for all $(i,j) \in \mathcal{I}_a$, and finally, that

$$\sum_{k,l\in\mathcal{I}_b} B_{tik}B_{tjl} = \bar{Q}_{tab} \tag{64}$$

is independent of $(i,j) \in \mathcal{I}_a$ for all $1 \le a, b \le d$ and $t = 1, 2, \ldots$. The last equation is equivalent to the row sum criterion for state space reduction (lumpability) of a time inhomogeneous Markov chain [6, 40]. This Markov chain runs backwards in time and characterizes the joint subpopulation history of a pair of genes, with transition probabilities $B_{tik}B_{tjl}$ and $\bar{Q}_{tab}$ before and after state space reduction.

It is shown in Appendix A that (62)–(64) lead to

$$f_{tij} = \bar{f}_{ta} \tag{65}$$

for all $(i,j) \in \mathcal{I}_a$ and $t = 1, 2, \ldots$, and that it suffices to consider the reduced column vectors $\bar{\boldsymbol{f}}_t = (\bar{f}_{ta})$ of length d, or equivalently, the corresponding reduced vectors $\bar{\boldsymbol{h}}_t = (\bar{h}_{ta})$ of gene diversities $\bar{h}_{ta} = 1 - \bar{f}_{ta}$. If these vectors are defined by drawing genes without replacement, they satisfy recursions

$$\begin{aligned} \bar{\boldsymbol{f}}_t &= (1-\mu)^2(\bar{\boldsymbol{D}}_t\bar{\boldsymbol{f}}_{t-1} - \bar{\boldsymbol{D}}_t\bar{\boldsymbol{1}} + \bar{\boldsymbol{1}}), \\ \bar{\boldsymbol{h}}_t &= (1-\mu)^2\bar{\boldsymbol{D}}_t\bar{\boldsymbol{h}}_{t-1} + \left(1-(1-\mu)^2\right)\bar{\boldsymbol{1}}, \end{aligned} \tag{66}$$

for $t = 1, 2, 3, \ldots$, analogous to (11), with $\bar{\boldsymbol{1}}$ a column vector of d ones, $\bar{\boldsymbol{D}}_t = (\bar{D}_{tab})$ a $d \times d$ matrix with elements

$$\begin{aligned} \bar{D}_{tab} &= \sum_{k,l\in\mathcal{I}_b} D_{tij,kl} \\ &\overset{(64)}{=} \bar{Q}_{tab}\left(1 - \frac{1}{2\bar{N}_{etb}}\right)^{\{b\le d_0\}}, \end{aligned} \tag{67}$$

independently of $i, j \in \mathcal{I}_a$.

If local census sizes, local effective sizes and migration rates are constant over time, as in Section 5, the above conditions simplify. The right hand sides of (62) take the form $\bar{N}_{ta} = \bar{N}_a$ and $\bar{N}_{eta} = \bar{N}_{ea}$ for $1 \le a \le d_0$, and the predicted gene identity recursion (66), when genes are drawn without replacement, reads

$$\bar{\boldsymbol{f}}_t = (1-\mu)^2(\bar{\boldsymbol{D}}\bar{\boldsymbol{f}}_{t-1} - \bar{\boldsymbol{D}}\bar{\boldsymbol{1}} + \bar{\boldsymbol{1}}), \tag{68}$$

since $\bar{\boldsymbol{D}}_t = \bar{\boldsymbol{D}} = (\bar{D}_{ab})$ does not depend on t.

Example 6 (Island model). For the island model [59,95,115], the forward migration rates are

$$M_{ki} = \begin{cases} 1-m, & i = k, \\ \frac{m}{(s-1)}, & i \ne k, \end{cases}$$

where m is the overall migration rate (59). We can use (40) to deduce that all subpopulations are equally large, i.e. $\boldsymbol{u} = (1,\dots,1)/s$, and therefore (41) implies $\boldsymbol{B} = \boldsymbol{M}$. We also assume that $N_{ei} = N_e$ for all i. The state space size can then be reduced from s^2 to $d = 2$, with $d_0 = d_1 = 1$ and

$$\begin{aligned} \mathcal{I}_1 &= \{(1,1),\dots,(s,s)\}, \\ \mathcal{I}_2 &= \{(i,j),\ 1 \le i \ne j \le s\}. \end{aligned}$$

It follows from (64) and (67) that

$$\bar{\boldsymbol{D}} = \begin{pmatrix} \left(1-\frac{1}{2N_e}\right)\bar{Q}_{11} & 1-\bar{Q}_{11} \\ \left(1-\frac{1}{2N_e}\right)\bar{Q}_{21} & 1-\bar{Q}_{21} \end{pmatrix}, \tag{69}$$

where

$$\begin{aligned} \bar{Q}_{11} &= \sum_{k=1}^{s} B_{ik}^2 = (1-m')^2 + \frac{2m' - (m')^2}{s}, \\ \bar{Q}_{21} &\overset{i\ne j}{=} \sum_{k=1}^{s} B_{ik}B_{jk} = \frac{m'(2-m')}{s} \end{aligned}$$

and $m' = sm/(s-1)$. Inserting (69) into (68), we obtain the same predicted gene identity recursion for two genes drawn without replacement as in [51,65] and [84], but note that these authors use the opposite notation for m and m'.

The reduced state space analogues of the weight vectors $\boldsymbol{W}_T$ and $\boldsymbol{W}_S$ for two genes drawn according to sampling schemes T and S, are $\bar{\boldsymbol{W}}_T = (\bar{W}_{Ta};\ 1 \le a \le d)$ and $\bar{\boldsymbol{W}}_S = (\bar{W}_{Sa};\ 1 \le a \le d)$ respectively, with elements

$$\begin{aligned} \bar{W}_{Ta} &= \sum_{(i,j)\in\mathcal{I}_a} w_i w_j, \\ \bar{W}_{Sa} &= 1_{\{a\le d_0\}} \sum_{i;(i,i)\in\mathcal{I}_a} w_i. \end{aligned} \tag{70}$$

When (65) holds, we can use $\bar{\boldsymbol{W}}_T$ and $\bar{\boldsymbol{W}}_S$ to express the predicted coefficient of gene differentiation (20), equivalently, as

$$g_{STt}([0,t]) = \frac{(\bar{\boldsymbol{W}}_S - \bar{\boldsymbol{W}}_T)\bar{\boldsymbol{f}}_t}{1 - \bar{\boldsymbol{W}}_T\bar{\boldsymbol{f}}_t}. \tag{71}$$

To guarantee that g_{STt} is non-negative, it is necessary to define $\bar{\boldsymbol{f}}_t$ and $\bar{\boldsymbol{h}}_t$ by drawing genes without replacement, as motivated in

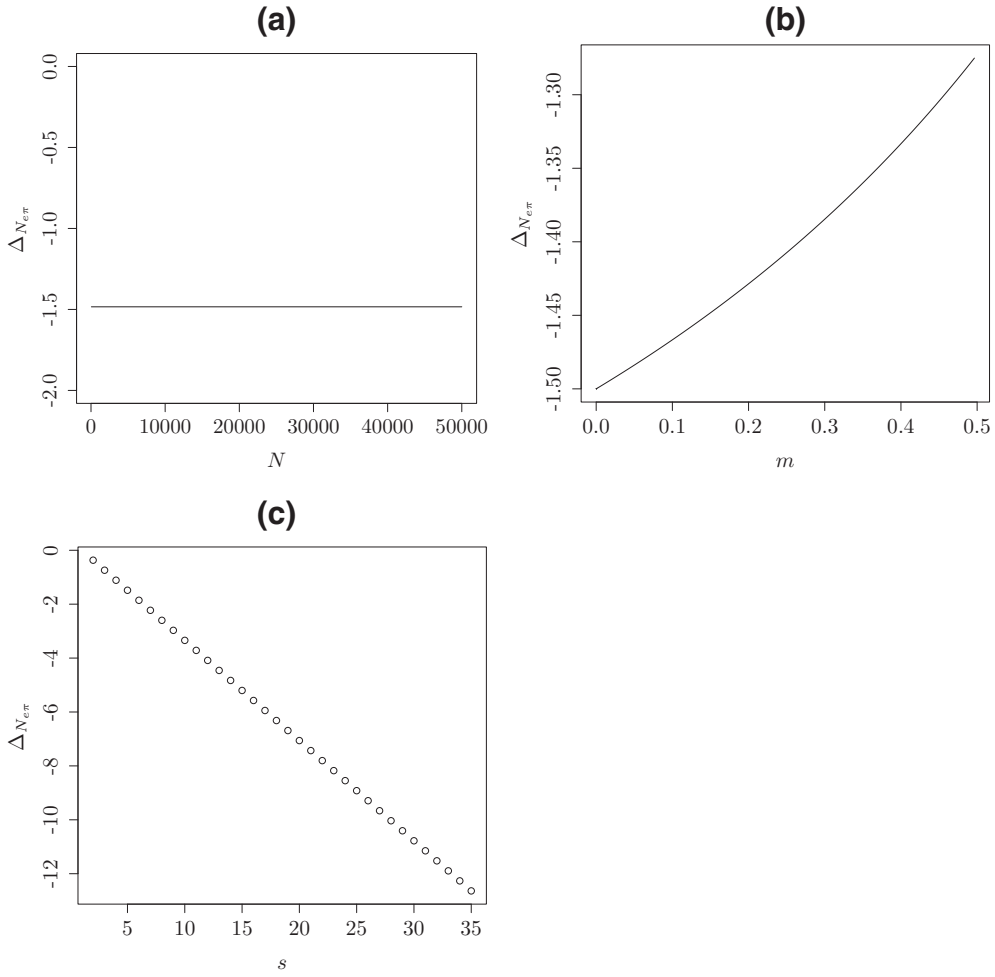

Fig. 7. The difference $\Delta N_{e\pi} = N_{e\pi} - N_{e\pi}^{\text{appr}}$ between exact and approximate nucleotide diversity effective sizes (72) and (73), for an island model without mutations ($\mu = 0$), as a function of a) N, b) m, and c) s. The parameters held constant have values $s = 5$, $m = 0.05$ and $N/s = N_e = 10,000$ in all subplots. In a), $\Delta N_{e\pi}$ attains a value of -1.48, almost independently of the population size, whereas in c), $\Delta N_{e\pi}$ is roughly proportional to s.

Section 3.4. This requires state space reduced analogues of $\boldsymbol{A}_t$ and (8), see Appendix A.

It is also possible to reexpress the effective population sizes in (28), (32) and (35) by replacing $\boldsymbol{W}_T$, $\boldsymbol{D}_t$, and $\boldsymbol{A}_t$ with their reduced state space analogues.

Example 7 (**Island model, contd.**). Continuing Example 6, if subpopulations are assigned the same weight (15), it follows from (70) that $\bar{\boldsymbol{W}}_T = (1/s, (s-1)/s)$ and $\bar{\boldsymbol{W}}_S = (1, 0)$, and therefore the predicted coefficient of gene differentiation (71) equals

$$g_{STt}([0,t]) = \frac{\frac{s-1}{s}(\bar{f}_{t1} - \bar{f}_{t2})}{1 - \left(\frac{1}{s}\bar{f}_{t1} + \frac{s-1}{s}\bar{f}_{t2}\right)}.$$

The nucleotide diversity effective size (55) can be written as

$$N_{e\pi} = \frac{1}{2}\bar{\boldsymbol{W}}_T(\boldsymbol{I} - \bar{\boldsymbol{D}})^{-1}\bar{\boldsymbol{1}} \tag{72}$$

for the island model when state space reduction is employed. Nei and Takahata [70] derived an explicit approximation

$$N_{e\pi}^{\text{appr}} = N\left(1 + \frac{(s-1)^2}{4Nms}\right) \tag{73}$$

of (72) when $N_{ei} = N_e = N/s$ is large and uniform weights (44) are used. Wakeley [99] derived a similar formula for the coalescence effective size N_{eC} when the number of subpopulations s is large as well. It is seen in Fig. 7 that (73) is a very good approximation of (72), with a relative error that is inversely proportional to the population size, whereas it only depends marginally on s and m. For instance, the relative error is between 1×10^{-5} and 2×10^{-5} when $N_e = 10,000$.

Example 8 (**Circular stepping stone model**). In natural populations, migration is often restricted to neighboring subpopulations. Kimura [41] proposed a class of stepping stone models with this feature, and its properties were further studied by Kimura and Weiss [44], Weiss and Kimura [109], Maruyama [58], and Durrett [19]. The subpopulations of the circular stepping stone model are located along the perimeter of a circle, and migration is only possible to the two neighbors, i.e.

$$M_{ki} = \begin{cases} 1-m, & i = k, \\ \frac{m}{2}, & i = k \pm 1, \\ 0, & \text{otherwise}, \end{cases}$$

where m is the overall migration rate (59), and addition is modulo s. By symmetry, we deduce from (40) that all subpopulations are equally large, so that $\boldsymbol{u} = (1, \ldots, 1)/s$ and $\boldsymbol{B} = \boldsymbol{M}$ because of (41). We also assume that the local size $N_{ek} = N_e$ is the same for all subpopulations k. The state space size can then be reduced from s^2 to $d = s$, with $d_0 = 1, d_1 = d - 1$ and

$$\mathcal{I}_a = \{(i,j);\ i - j = a - 1 \text{ modulo } s\}, \quad a = 1, \ldots, s.$$

It follows from (64) and (67) that

$$\bar{D}_{ab} = \left(1-\frac{1}{2N_e}\right)^{\{b=1\}}\bar{Q}_{ab} \overset{s\geq 5}{=} \left(1-\frac{1}{2N_e}\right)^{\{b=1\}}\cdot\begin{cases}(1-m)^2+\frac{m^2}{2}, & b=a,\\ m(1-m), & b=a\pm 1,\\ \frac{m^2}{4}, & b=a\pm 2,\\ 0, & |b-a|>2.\end{cases} \tag{74}$$

When m, μ and $1/N_e$ are all small, we may drop all quadratic terms m^2, μ^2, m/N_e and μ/N_e. The recursion (68), with $\bar{\boldsymbol{D}}=(\bar{D}_{ab})$ as in (74), then simplifies to those in [57, p. 89] and [19, p. 162–163]. The equilibrium solution of the approximate recursion is provided in Theorem 5.2 of [19], and the corresponding exact asymptotic solution of (66) can be written as

$$\bar{\boldsymbol{f}}_\infty = (1-\mu)^2(\bar{\boldsymbol{I}}-(1-\mu)^2\bar{\boldsymbol{D}})^{-1}(\bar{\boldsymbol{1}}-\bar{\boldsymbol{D}}\bar{\boldsymbol{1}}),$$

with $\bar{\boldsymbol{I}}$ the identity matrix of order s. See also [3] for the exact recursion and asymptotic equilibrium solution of the infinite ($s=\infty$) stepping stone model. Results in Appendix A, (57) and (58) imply

$$\lambda_{\max}(\bar{\boldsymbol{D}})=\lambda_{\max}(\boldsymbol{D}) \Longrightarrow N_{eE}=\frac{1}{2(1-\lambda_{\max}(\bar{\boldsymbol{D}}))}, \tag{75}$$

for any state space reduced model. Maruyama [58] gave asymptotic expressions for N_{eE} for the circular stepping stone model under two different scenarios; large local effective population sizes N_e and small migration rates m. Wang and Caballero [103] combined these two approximations into one single formula

$$N_{eE}\approx sN_e+\frac{s^2}{2m\pi^2}$$

that approximates (75). If uniform subpopulations weights (15) are used, it follows from (70) that $\bar{\boldsymbol{W}}_T=(1/s,\dots,1/s)$ and $\bar{\boldsymbol{W}}_S=(1,0,\dots,0)$, so that the predicted coefficient of gene differentiation (71) is

$$g_{STt}([0,t])=\frac{\frac{s-1}{s}\bar{f}_{t1}-\frac{1}{s}\sum_{a=2}^{s}\bar{f}_{ta}}{1-\frac{1}{s}\sum_{a=1}^{s}\bar{f}_{ta}}.$$

Example 9 (Hierarchical island model). This model was introduced by Carmelli and Cavalli-Sforza [9], and further treated by Sawyer and Felsenstein [87], Slatkin and Voelm [92] and Hössjer [34]. The subpopulations $i=(i_1,i_2)$ are divided into s_1 regions of equal size s_2, with i_1 the region number and i_2 the subpopulation number within a region. The total migration probability $m=m_w+m_b$ consists of two parts; the probability m_w to migrate within a region, divided equally $m_w/(s_2-1)$ between its subpopulations, or a probability m_b to migrate between regions, divided equally $m_b/((s_1-1)s_2)$ between all subpopulations in the other regions. Hence

$$M_{(k_1,k_2),(i_1,i_2)} = (1-m_w-m_b)1_{\{(i_1,i_2)=(k_1,k_2)\}} + \frac{m_w}{s_2-1}1_{\{i_1=k_2,i_2\neq k_2\}} + \frac{m_b}{(s_1-1)s_2}1_{\{i_1\neq k_1\}}. \tag{76}$$

By symmetry, if follows that all subpopulations are equally large, so that $\boldsymbol{u}=(1,\dots,1)/s$ and $\boldsymbol{B}=\boldsymbol{M}$. We also assume that the local effective size $N_{ei}=N_e$ is the same for all subpopulations. The state space size can then be reduced from s^2 to $d=3$, with $d_0=1$, $d_1=2$ and

$$\mathcal{I}_1=\{(i_1,i_2),(i_1,i_2);\ 1\leq i_1\leq s_1, 1\leq i_2\leq s_2\},$$
$$\mathcal{I}_2=\{(i_1,i_2),(i_1,j_2);\ 1\leq i_1\leq s_1, 1\leq i_2\neq j_2\leq s_2\},$$
$$\mathcal{I}_3=\{(i_1,i_2),(j_1,j_2);\ 1\leq i_1\neq j_1\leq s_1, 1\leq i_2,j_2\leq s_2\}.$$

As for the island and stepping stone models we have that

$$\bar{D}_{ab}=\left(1-\frac{1}{2N_e}\right)^{\{b=1\}}\bar{Q}_{ab}$$

for $1\leq a,b\leq 3$, where $\bar{Q}_{ab}$ are functions of m_w, m_b, s_1 and s_2 that can be derived from (64), (76) and the fact that $\boldsymbol{B}=\boldsymbol{M}$.

If all subpopulations have the same weight (15), it follows from (70) that $\bar{\boldsymbol{W}}_T=(1/s,1/s_1-1/s,1-1/s_1)$ and $\bar{\boldsymbol{W}}_S=(1,0,0)$, so that the predicted coefficient of gene differentiation (71) is

$$g_{STt}([0,t])=\frac{\frac{s-1}{s}\bar{f}_{t1}-\left(\frac{1}{s_1}-\frac{1}{s}\right)\bar{f}_{t2}-\left(1-\frac{1}{s_1}\right)\bar{f}_{t3}}{1-\frac{1}{s}\bar{f}_{t1}-\left(\frac{1}{s_1}-\frac{1}{s}\right)\bar{f}_{t2}-\left(1-\frac{1}{s_1}\right)\bar{f}_{t3}}.$$

7. Discussion

7.1. Summary and conclusions

In this paper we introduce a class of models for a diploid, monoecious and subdivided population with temporally varying subpopulation sizes. Exact matrix analytic recursion formulas are derived for predicted gene diversities/gene identities, identity by descent and coalescence probabilities, and standardized covariances of allele frequency change. From this we obtain exact expressions for predictions of the coefficient of gene differentiation (g_{ST}) and a number of different types of effective sizes N_e. We also consider general ways of weighting subpopulations in order to account for long and short term effects, local and global features, and develop a general scheme for state space reduction.

We argue that in order to adequately summarize the most important properties of a subdivided population, the dynamic behavior of g_{ST} and (certain versions of) N_e should be reported as a function of time. Indeed, the examples of Section 5 reveal that single values of g_{ST} and global N_e may be very wrong if long term equilibrium conditions are assumed, and single values of local N_e as well, if subpopulation isolation is assumed.

One aspect of our work is to put various types of the effective sizes into a general framework. These are defined forwards or backwards over time intervals of various lengths, with subpopulations weighted in different ways and pairs of genes drawn with or without replacement. Although in practice the latter distinction is not crucial, unless some subpopulation is very small, it clarifies the relation between the inbreeding and variance effective sizes N_{eI} and N_{eV}, since the latter is essentially a version of the former with genes drawn with rather than without replacement. As one implication of this we could show very generally that N_{eI} lags N_{eV} by one unit of time for populations of varying size, thereby confirming results for homogeneous populations [43]. The nucleotide diversity effective size $N_{e\pi}$ looks backwards in terms of expected coalescence probabilities, whereas the eigenvalue effective size N_{eE} looks forwards and quantifies the long term rate at which inbreeding increases (with or without replacement). It is only defined for constant or regularly changing populations, and is the only notion of effective size that is independent of the subpopulation weighting scheme. Both N_{eI} and N_{eV} are defined over time intervals of finite length t, and although they both converge to N_{eE} as t increases, the convergence rate $O(1/t)$ is very slow, unless equilibrium conditions prevail at the beginning of the time interval, or if reproductive weights are used. In general it is therefore possible to quantify long term genetic changes from short intervals with N_{eI} and N_{eV}, only with reproductive weights.

Our focus has been to compute quantities exactly, not relying on large population asymptotics. The coalescence effective size (N_{eC}) exists when the ancestry of a sample converges to Kingman's coalescent [45] as the population size grows. Only in this case it is possible to summarize the rate of genetic loss by one single number, and for this reason [88] advocate N_{eC}. However, two finite populations that are approximated by Kingman ancestries can still behave differently, and for other populations, for which N_{eC} does not exist, it is still important to quantify the dynamics of genetic loss, using some other notion of

effective size. For instance, it is shown in [35] that N_{eE} is a more general concept than N_{eC}, since the latter is an asymptotic limit of N_{eE} for structured populations of growing size with a limiting coalescence ancestry of Kingman type.

7.2. Practical conservation genetics aspects

The analytical work presented here is useful for research in the fields of conservation biology and conservation genetics, and we intend to present such applications in forthcoming publications that are directed towards workers of those fields. For instance, the algorithms presented here have been implemented in a user friendly software (GESP) for genetic exploration of structured populations [74], which we hope will be a helpful tool for conservation biologists, facilitating investigation of short and long term inbreeding and genetic divergence when populations are connected through various rates of gene flow. For example, our framework enables exploration of how the conservation genetic status of a population system might be affected by reductions and expansions of subpopulations with various degrees of connectivity. Such studies are of relevance to many practical situations in the management of species in terrestrial as well as aquatic environments such as the Fennoscandic wolf population system [47], and for keystone ecological species of the Baltic Sea. Further, the opportunity of describing effective population size of substructured populations constitutes a basis for further development of general conservation genetics guidelines and monitoring schemes.

7.3. Future perspectives

The results of this paper could be extended in a number of ways. First, the reproduction model of Section 2 could be modified in order to incorporate diploid two sex models with gene identities that correspond to inbreeding coefficients within individuals or coefficients of consanguinity between different individuals, in the same or different subpopulations. Previous work includes the gene identity recursions in Section 3.8 of [18], the inbreeding recursions for age structured models in [13], and the inbreeding recursions for an island model of diploid monoecious or dioecious individuals [12,101,102].

Second, real data estimates of our novel expressions for N_e and g_{ST} should be developed, employing for instance methods described in the review papers of Luikart et al. [55] and Levyiang and Hamilton [50]. Whereas the sampling scheme of Section 3.3 was a theoretical construct, real data estimates requires sampling of a number of individuals for all subpopulations i that have positive weights w_i. For instance, the temporal method is used to estimate $N_{eV}([0,t])$ from genetic data sampled at two time points $r \in \{0,t\}$ at a number of genetic markers $l = 1,\dots,L$, see [69,78,106] for homogeneous populations, and [37,108] for structured populations. If all markers are biallelic, estimates $\hat{P}_{ri}^{(l)}$ and

$$\hat{P}_r^{(l)} = \sum_{i=1}^{s} w_i \hat{P}_{ri}^{(l)}, \tag{77}$$

are provided for each time point r, of the frequencies of one of the two alleles at all loci l, in subpopulation i and the whole population respectively. This is used in [75] to extend an approach of [38] for homogeneous populations by estimating (34), and hence also (35), from the genetic drift of (77), averaged over several loci. It turns out that the choice of subpopulation weights w_i is important, and the long term genetic drift (as quantified by N_{eE}) can be estimated even from short time intervals with reproductive weights (45), for a population of constant size, see [73].

Third, one may study the effect of mutation on effective size, and definitions (25), (28) or (30) of the inbreeding effective size are special cases of

$$N_{eI}([t_0,t]) = \begin{cases} \dfrac{1}{2\left(1-\left(\frac{1-f_{Tt}}{1-f_{Tt_0}}\right)^{1/(t-t_0)}\right)}, & f_{Tt} > f_{Tt_0}, \\ \text{NaN}, & f_{Tt} \le f_{Tt_0}, \end{cases} \tag{78}$$

with an identity by descent probability f_{Tt} of the whole population in generation t that allows for mutations. This is different though from the heterozygosity effective size N_{eh} of [19, p. 154] or the coalescence effective size N_{eC} of [100], who included mutation as a source of genetic change accounted for, not as an uncorrected confounder. A further extension of N_{eI} would be to allow for selection as well.

Fourth, the whole predictive distribution of G_{STt} is sometimes of interest, not only a predictor g_{STt} of it, see [48,49,81] for work along these lines for the island and two-dimensional stepping stone models. It would be challenging to generalize such methods to arbitrary migration schemes. On the other hand the multilocus extension

$$G_{STt} = \frac{\sum_{l=1}^{L} H_{Tt,l} - \sum_{l=1}^{L} H_{St,l}}{\sum_{l=1}^{L} H_{Tt,l}}$$

of the coefficient of gene differentiation in [64], will be more concentrated around g_{STt} the larger the number of loci L is, suggesting that g_{STt} is an adequate measure of subpopulation differentiation.

Fifth, for conservation genetics applications, it is well known that a bottleneck implies a transient loss of rare alleles, see [14,54,60] and [28]. It would be of interest to quantify some of the statistics of these papers, and other quantities that are functions of the allele frequency spectrum from multiple loci, analytically for subdivided populations.

Acknowledgements

Ola Hössjer was supported by the Swedish Research Council, contracts nr. 621-2008-4946 and 621-2013-4633, and the Gustafsson Foundation for Research in Natural Sciences and Medicine. Linda Laikre and Nils Ryman were funded by grants from the Swedish Environmental Protection Agency, the Swedish Research Council, the Swedish Research Council Formas, and the BONUS project BAMBI, the joint Baltic Sea research and development programme (Art185), funded jointly from the European Union's Seventh Programme for research, technological development and demonstration and from the Swedish Research Council Formas. The authors want to thank Lars Nørvang Anderson for providing some valuable references and two reviewers for very helpful comments that considerably improved the quality of the paper.

Appendix A. Extensions of theory and proofs

Proof of (6) and (10). If genes are drawn with replacement, we first show

$$0 \le F_{tij} \le \sqrt{F_{tii}F_{tjj}}, \tag{79}$$

for any pair of subpopulations i and j. It is clear from the definition of F_{tij} in (3) that the left inequality of (79) holds, since all allele frequencies P_{tia} are non-negative. Moreover, this inequality is sharp since $F_{tij} = 0$ if $i \neq j$ and at most one of P_{tia} and P_{tja} is positive for any allele a. In order to prove the right inequality of (79), we assume without loss of generality that $F_{tii} \ge F_{tjj}$. Let $\mathcal{A}_{ti} = \{a;\ 1 \le a \le n_t, P_{tia} > 0\}$ denote the set of alleles in subpopulation i, and put $F'_{tjj} = \sum_{a\in\mathcal{A}_{ti}} P_{tja}^2 \le F_{tjj}$. Then

$$\begin{aligned} F_{tij} &= \sum_{a\in\mathcal{A}_{ti}} P_{tia}P_{tja} \\ &\le \sqrt{\sum_{a\in\mathcal{A}_{ti}} P_{tia}^2} \times \sqrt{\sum_{a\in\mathcal{A}_{ti}} P_{tja}^2} \\ &= \sqrt{F_{tii}} \times \sqrt{F'_{tjj}} \\ &\le \sqrt{F_{tii}} \times \sqrt{F_{tjj}}, \end{aligned}$$

using Cauchy Schwarz inequality in the second step. In order to prove that the right hand side of (79) can be attained for any F_{tii} and F_{tjj}, we first choose allele frequencies so that P_{tja}/P_{tia} is constant for $a \in \mathcal{A}_{tia}$. Then the fourth step holds with equality asymptotically, in the limit of large populations, if $n_t - |\mathcal{A}_{ti}| \to \infty$ and $\max_{a \notin \mathcal{A}_{ti}} P_{tja} \to 0$. We then obtain (6) from (79) and Cauchy-Schwarz inequality, as

$$\begin{aligned} f_{tij} &= E_0(F_{tij}) \\ &\le E_0\left(\sqrt{F_{tii}} \times \sqrt{F_{tjj}}\right) \\ &\le \sqrt{E_0(F_{tii})} \times \sqrt{E_0(F_{tjj})} \\ &= \sqrt{f_{tii} f_{tjj}}. \end{aligned}$$

Finally, it follows from (9) that $f_{tij}^{\text{without}} = f_{tij}^{\text{with}}$ is the same if $i \neq j$, whether the two genes are drawn with or without replacement, whereas $f_{tii}^{\text{without}} = 2N_{ti} f_{tii}^{\text{with}}/(2N_{ti}-1) - 1/(2N_{ti}-1)$. Together with (6), this proves (10). □

Proof of (8). We first verify the lower part of (8) when $\mu = 0$. Assume $t \ge 1$ and let E_{t-1} denote expectation conditionally on allele frequencies at generation $t-1$. By the definition of the reproduction scheme in Section 2,

$$\begin{aligned} E_{t-1}(H_{tij}) = &\left(1 - \frac{1}{2N_{ti}}\right)^{\{i=j\}} \\ &\times \sum_{k,l=1}^{s} B_{tik} B_{tjl} \left(1 - \frac{1}{2N_{e,t-1,k}}\right)^{\{k=l\}} \frac{H_{t-1,kl}}{\left(1 - \frac{1}{2N_{t-1,k}}\right)^{\{k=l\}}}, \end{aligned}$$

since $(1-1/(2N_{ti}))^{\{i=j\}}$ is the probability that the two genes drawn from subpopulations i and j in generation t are different, $B_{tik}B_{tjl}$ is the probability that the two parents of two different genes from i and j come from subpopulations k and l, $(1-1/(2N_{e,t-1,k}))^{\{k=l\}}$ is the probability that the two parental gametes in k and l originate from different genes in the parental generation $t-1$, and $H_{t-1,kl}/(1-1/(2N_{t-1,k}))^{\{k=l\}}$ is the gene diversity of the two parental gametes, given that they originate from different genes in subpopulations k and l of generation $t-1$.

Taking expectation E_0 on both sides of the last displayed equation,

$$\begin{aligned} h_{tij} = &\left(1 - \frac{1}{2N_{ti}}\right)^{\{i=j\}} \\ &\times \sum_{k,l=1}^{s} B_{tik} B_{tjl} \left(1 - \frac{1}{2N_{e,t-1,k}}\right)^{\{k=l\}} \frac{h_{t-1,kl}}{\left(1 - \frac{1}{2N_{t-1,k}}\right)^{\{k=l\}}}, \end{aligned}$$

proving the lower part of (8) when $\mu = 0$. For any μ, we derive (8);

$$\begin{aligned} h_{tij} = &(1-\mu)^2 \times (\boldsymbol{A}_t \boldsymbol{h}_{t-1})_{ij} \\ &+ (1-(1-\mu)^2) \times \left(1 - \frac{1_{\{i=j\}}}{2N_{ti}}\right) + 0 \times \frac{1_{\{i=j\}}}{2N_{ti}} \end{aligned}$$

by conditioning on whether the same gene (with probability $1_{\{i=j\}}/(2N_{ti})$) or not is drawn, and in the latter case whether at least one of the two genes have mutated since the last generation (with probability $1-(1-\mu)^2$) or not. Since $\boldsymbol{f}_t = \boldsymbol{1} - \boldsymbol{h}_t$, we then obtain the upper part of (8) from the lower. □

Proof of (11). In order to prove the lower part of (11), we argue as in the proof of (8) and initially assume $\mu = 0$. Since the two genes of subpopulations i and j in generation t are drawn without replacement,

$$E_{t-1}(H_{tij}) = \sum_{k,l=1}^{s} B_{tik} B_{tjl} \left(1 - \frac{1}{2N_{e,t-1,k}}\right)^{\{k=l\}} H_{t-1,kl},$$

and the rest of the proof is completely analogous to that of (8). For general μ, we condition on whether there is at least mutation between generations $t-1$ and t or not, and find that

$$\boldsymbol{h}_{tij} = (1-\mu)^2 \times (\boldsymbol{D}_t \boldsymbol{h}_{t-1})_{ij} + (1-(1-\mu)^2) \times 1,$$

since the expected gene diversity is $(\boldsymbol{D}_t \boldsymbol{h}_{t-1})_{ij}$ if none of the two genes mutates between $t-1$ and t, and 1 if at least one of them does. This proves the lower part of (11), and the upper part follows since $\boldsymbol{f}_t = \boldsymbol{1} - \boldsymbol{h}_t$. □

Non-negativity of (17). When two genes are drawn with replacement in the definitions of H_{Tt} and H_{St}, the numerator of (17), the so called gene differentiation between subpopulations, satisfies

$$\begin{aligned} D_{STt} &= H_{Tt} - H_{St} \\ &= \sum_{i \neq j} w_i w_j D_{tij} \\ &= \sum_{a=1}^{n_t} \sum_{i=1}^{s} w_i (P_{tia} - P_{t\cdot a})^2 \\ &\ge 0, \end{aligned}$$

where $P_{t\cdot a} = \sum_i w_i P_{tia}$, and $D_{tij} = H_{tij} - (H_{tii} + H_{tjj})/2$ is the non-negative gene differentiation between subpopulations i and j.

Proof of (27). Suppose $\mathcal{S} = \{i\}$. Then $\boldsymbol{W}_T$ is a row vector with one in position (i,i) and zeros elsewhere, so that (25) simplifies to

$$N_{el}([t,t+1]) = \begin{cases} \dfrac{1}{2\left(1 - \left(\frac{\sum_{kl} D_{t+1,ii,kl}(1-f_{tkl})}{1-f_{tii}}\right)\right)}, & f_{t+1,ii} > f_{tii}, \\ \text{NaN}, & f_{t+1,ii} \le f_{tii}, \end{cases} \tag{80}$$

for a time interval of length 1. If additionally i is isolated, $B_{t+1,ii} = 1$ and

$$D_{t+1,ii,kl} = 1_{\{(k,l)=(i,i)\}} \left(1 - \frac{1}{2N_{eti}}\right). \tag{81}$$

Inserting (81) into (80), we arrive at (27). □

Proof of (34). We will prove that $\boldsymbol{f}_t = (f_{tij}^{\text{cov}})$ satisfies the recursion

$$\boldsymbol{f}_t = \boldsymbol{A}_t \boldsymbol{f}_{t-1} - \boldsymbol{A}_t \boldsymbol{1} + \boldsymbol{1}, \tag{82}$$

a special case of the upper equation of (8) with $\mu = 0$. Indeed, since the gene is biallelic ($n_t = 2$), it follows from (4) that the gene diversity between two subpopulations i and j in generation t simplifies to

$$H_{tij} = P_{ti}(1-P_{tj}) + P_{tj}(1-P_{ti}). \tag{83}$$

Let $\boldsymbol{P}_t = (P_{t1}, \ldots, P_{ts})'$ be the vector of frequencies of Allele 1 in all subpopulations. A consequence of the definition of the reproduction scenario in Section 2 is that $E(\boldsymbol{P}_t | \boldsymbol{P}_{t-1}) = \boldsymbol{B}_t \boldsymbol{P}_{t-1}$. Since $\boldsymbol{P}_0 = P_0 \boldsymbol{1}_s$ is assumed, where $\boldsymbol{1}_s$ is a column vector of s ones, it follows by induction with respect to t that $E_0(\boldsymbol{P}_t) = P_0 \boldsymbol{1}_s$ for any $t = 1, 2, \ldots$. Taking expectation on both sides of (83) and invoking the lower part of (5), we deduce

$$\begin{aligned} h_{tij} &= E_0(H_{tij}) \\ &= E_0\left(P_{ti}(1-P_{tj}) + P_{tj}(1-P_{ti})\right) \\ &= 2P_0(1-P_0) - 2\text{Cov}_0(P_{ti}, P_{tj}) \\ &= 2P_0(1-P_0)(1-f_{tij}), \end{aligned}$$

where in the last step we used the definition of $f_{tij} = f_{tij}^{\text{cov}}$ in (33). From this, and the special case $\boldsymbol{h}_t = \boldsymbol{A}_t \boldsymbol{h}_{t-1}$ of the recursion for $\boldsymbol{h}_t$ in the lower part of (8), when $\mu = 0$, it follows that

$$\begin{aligned} \boldsymbol{f}_t &= \boldsymbol{1} - \boldsymbol{h}_t/(2P_0(1-P_0)) \\ &= \boldsymbol{1} - \boldsymbol{A}_t \boldsymbol{h}_{t-1}/(2P_0(1-P_0)) \\ &= \boldsymbol{1} - \boldsymbol{A}_t(\boldsymbol{1} - \boldsymbol{f}_{t-1}) \\ &= \boldsymbol{A}_t \boldsymbol{f}_{t-1} - \boldsymbol{A}_t \boldsymbol{1} + \boldsymbol{1}, \end{aligned}$$

and this completes the proof of (82). Since the allele frequencies of all subpopulations are the same in generation $t = 0$, we must have $\boldsymbol{f}_0 = \boldsymbol{0}$. In conjunction with (82) this leads to $\boldsymbol{f}_t = \boldsymbol{1} - \boldsymbol{A}_t \cdot \ldots \cdot \boldsymbol{A}_1 \boldsymbol{1}$, and multiplying this vector with $\boldsymbol{W}_T$, we finally arrive at (34). □

Proof of (58). Write $\boldsymbol{A}^t = (A^{(t)}_{ij,kl})$ and $\boldsymbol{D}^t = (D^{(t)}_{ij,kl})$. We first prove that

$$A^{(t)}_{ij,kl} = \frac{1-\delta_{ij}}{1-\delta_{kl}} D^{(t)}_{ij,kl} \tag{85}$$

by induction with respect to $t = 1, 2, \ldots$, with δ_{ij} as defined below (47). When $t = 1$, (85) follows directly from the definitions of $\boldsymbol{A}$ and $\boldsymbol{D}$ in (47) and (49). Suppose next that (85) has been established up to $t \geq 1$. Then

$$\begin{aligned} A^{(t+1)}_{ij,kl} &= \sum_{mn} A_{ij,mn} A^{(t)}_{mn,kl} \\ &= \sum_{mn} \left(\frac{1-\delta_{ij}}{1-\delta_{mn}} D_{ij,mn} \right) \left(\frac{1-\delta_{mn}}{1-\delta_{kl}} D^{(t)}_{mn,kl} \right) \\ &= \frac{1-\delta_{ij}}{1-\delta_{kl}} \sum_{mn} D_{ij,mn} D^{(t)}_{mn,kl} \\ &= \frac{1-\delta_{ij}}{1-\delta_{kl}} D^{(t+1)}_{ij,kl}, \end{aligned}$$

so that (85) holds for $t+1$, completing the induction proof of (85). It follows from Perron Frobenius' Theorem that

$$\begin{aligned} \boldsymbol{A}^t &= \lambda^t \boldsymbol{r}\boldsymbol{\rho} + o(\lambda^t), \\ \boldsymbol{D}^t &= \tilde{\lambda}^t \tilde{\boldsymbol{r}}\tilde{\boldsymbol{\rho}} + o(\tilde{\lambda}^t), \end{aligned} \tag{86}$$

as $t \to \infty$, where $\lambda = \lambda_{\max}(\boldsymbol{A})$ is the largest eigenvalue of $\boldsymbol{A}$, with corresponding $s^2 \times 1$ right eigenvector $\boldsymbol{r} = (r_{ij})$, and $1 \times s^2$ left eigenvector $\boldsymbol{\rho} = (\rho_{kl})$. Analogously, $\tilde{\lambda} = \lambda_{\max}(\boldsymbol{D})$ is the largest eigenvalue of $\boldsymbol{D}$, with accompanying right and left eigenvectors $\tilde{\boldsymbol{r}} = (\tilde{r}_{ij})$ and $\tilde{\boldsymbol{\rho}} = (\tilde{\rho}_{kl})$. Comparing (85) and (86), it is clear that $\lambda = \tilde{\lambda}$, and the leading right and left eigenvectors of $\boldsymbol{A}$ and $\boldsymbol{D}$ can normalized so that $r_{ij} = \tilde{r}_{ij}(1-\delta_{ij})$ and $\rho_{kl} = \tilde{\rho}_{kl}/(1-\delta_{kl})$, and this completes the proof of (58).

When the eigenvalues $\lambda = \lambda_1 > \lambda_2 > \ldots > \lambda_{s^2}$ of $\boldsymbol{A}$ are all distinct, a Jordan decomposition of $\boldsymbol{A}$ implies that right and left eigenvectors $\boldsymbol{r}_a = (r_{a,ij};\ 1 \leq i,j \leq s)$ and $\boldsymbol{\rho}_a = (\rho_{a,ij};\ \leq i,j \leq s)$ with eigenvalues λ_a exist for each $1 \leq a \leq s^2$. It follows easily from (85), with $t = 1$, that $\tilde{\boldsymbol{r}}_a = (\tilde{r}_{a,ij};\ 1 \leq i,j \leq s)$ and $\tilde{\boldsymbol{\rho}}_a = (\tilde{\rho}_{a,ij};\ \leq i,j \leq s)$ are right and left eigenvectors of $\boldsymbol{D}$ with the same eigenvalue λ_a, provided $r_{a,ij} = \tilde{r}_{a,ij}(1-\delta_{ij})$ and $\rho_{a,kl} = \tilde{\rho}_{a,kl}/(1-\delta_{kl})$. Hence the whole spectrum of eigenvalues of $\boldsymbol{A}$ and $\boldsymbol{D}$ is the same. □

Proof of (61). When subpopulation sizes and migration rates are constant over time, it follows from (28), (30) and (35) that

$$\begin{aligned} N_{el}([0,t]) &\overset{(25)}{=} 1/(2(1-((\boldsymbol{W}_T\boldsymbol{D}^t(\boldsymbol{1}-\boldsymbol{f}_0))/(\boldsymbol{W}_T(\boldsymbol{1}-\boldsymbol{f}_0)))^{1/t})), \\ N_{el}([0,t]) &\overset{(30)}{=} 1/(2(1-((\boldsymbol{W}_T\boldsymbol{A}^t(\boldsymbol{1}-\boldsymbol{f}_0))/(\boldsymbol{W}_T(\boldsymbol{1}-\boldsymbol{f}_0)))^{1/t})), \\ N_{eV}([0,t]) &\overset{(35)}{=} 1/(2(1-(\boldsymbol{W}_T\boldsymbol{A}^t\boldsymbol{1})^{1/t})). \end{aligned}$$

We need to prove that the right hand sides of all these three formulas converge to (28) as $t \to \infty$. We confine ourselves with (30), since (35) is a special case of this formula, with $\boldsymbol{f}_0 = \boldsymbol{0}$, and since (25) is analogous to (30), replacing $\boldsymbol{A}$ by $\boldsymbol{D}$ everywhere. Recalling that $\boldsymbol{h}_0 = \boldsymbol{1} - \boldsymbol{f}_0$, we find that

$$\begin{aligned} (\boldsymbol{W}_T\boldsymbol{A}^t\boldsymbol{h}_0/(\boldsymbol{W}_T\boldsymbol{h}_0))^{1/t} &= (\boldsymbol{W}_T(\lambda^t\boldsymbol{r}\boldsymbol{\rho} + o(\lambda^t))\boldsymbol{h}_0/(\boldsymbol{W}_T\boldsymbol{h}_0))^{1/t} \\ &= \lambda((\boldsymbol{W}_T\boldsymbol{r})(\boldsymbol{\rho}\boldsymbol{h}_0)/(\boldsymbol{W}_T\boldsymbol{h}_0) + o(1))^{1/t} \\ &= \lambda(C + o(1))^{1/t} \\ &= \lambda + O(1/t) \end{aligned}$$

as $t \to \infty$. The remainder term vanishes when $(\boldsymbol{W}_T\boldsymbol{A}^t\boldsymbol{h}_0/(\boldsymbol{W}_T\boldsymbol{h}_0))^{1/t} = \lambda$, which happens when $\boldsymbol{W}_T = \boldsymbol{\rho}$, the left eigenvectors of $\boldsymbol{A}$ with eigenvalue λ, or when $\boldsymbol{h}_0 = \boldsymbol{r}$, the corresponding right eigenvector of $\boldsymbol{A}$. □

Reduced state space recursions. Assume first that two genes are drawn without replacement. To prove the upper part of (66), we start to show that f_{tij} is independent of $i,j \in \mathcal{I}_a$, as specified by (65) for $t = 0, 1, 2, \ldots$. When $t = 0$, (65) follows from (63). Assume $t \geq 1$ and that (65) holds for $t-1$. Pick $a \in \{1, \ldots, d\}$ and any $i,j \in \mathcal{I}_a$. The upper part of (11) implies

$$\begin{aligned} f_{tij} &= (1-\mu)^2 \left((\boldsymbol{D}_t\boldsymbol{f}_{t-1})_{ij} - (\boldsymbol{D}_t\boldsymbol{1})_{ij} + 1 \right) \\ &= (1-\mu)^2 \left(\sum_{k,l} D_{tij,kl}(f_{t-1,kl} - 1) + 1 \right) \\ &= (1-\mu)^2 \left(\sum_{b=1}^{d} (\bar{f}_{t-1,b} - 1) \sum_{k,l \in \mathcal{I}_b} D_{tij,kl} + 1 \right) \\ &= (1-\mu)^2 \left(\sum_{b=1}^{d} (\bar{f}_{t-1,b} - 1)\bar{D}_{tab} + 1 \right) \\ &= (1-\mu)^2 \left((\bar{D}_t\bar{\boldsymbol{f}}_{t-1})_a - (\bar{\boldsymbol{D}}_t\bar{\boldsymbol{1}})_a + 1 \right) \\ &=: \bar{f}_{ta}, \end{aligned}$$

and this completes the induction step, so that (65) is verified, as well as the upper part of (66). Finally, the lower part of (66) follows from the upper part, since $h_{tij} = \bar{h}_{ta} = 1 - \bar{f}_{ta}$ for $i,j \in \mathcal{I}_a$ and $a = 1, \ldots, d$.

When two genes are drawn with replacement, the gene identities and gene diversities will satisfy recursions

$$\begin{aligned} \bar{\boldsymbol{f}}_t &= (1-\mu)^2(\bar{\boldsymbol{A}}_t\bar{\boldsymbol{f}}_{t-1} - \bar{\boldsymbol{A}}_t\bar{\boldsymbol{1}} + \bar{\boldsymbol{1}}) + (1-(1-\mu)^2)\bar{\boldsymbol{\delta}}_t, \\ \bar{\boldsymbol{h}}_t &= (1-\mu)^2\bar{\boldsymbol{A}}_t\bar{\boldsymbol{h}}_{t-1} + (1-(1-\mu)^2)(\bar{\boldsymbol{1}} - \bar{\boldsymbol{\delta}}_t), \end{aligned} \tag{87}$$

for $t = 1, 2, \ldots$ that are reduced state space versions of the recursions in (8), with $\bar{\boldsymbol{A}}_t = (\bar{A}_{tab})$ a $d \times d$ matrix with elements

$$\begin{aligned} \bar{A}_{tab} &= \sum_{k,l \in \mathcal{I}_b} A_{tij,kl} \\ &= \left(1 - \frac{1}{2\bar{N}_{ta}}\right)^{\{a \leq d_0\}} \bar{Q}_{tab} \left(\frac{1 - \frac{1}{2\bar{N}_{etb}}}{1 - \frac{1}{2\bar{N}_{tb}}} \right)^{\{b \leq d_0\}}, \end{aligned}$$

for any $i,j \in \mathcal{I}_a$, with $\bar{\boldsymbol{\delta}}_t = (\bar{\delta}_{ta})$ a $d \times 1$ vector with $\bar{\delta}_{ta} = 1_{\{a \leq d_0\}}/(2\bar{N}_{ta})$. Formula (87) is proved as (66), using (8) instead of (11).

Proof of (75). Write $\bar{\boldsymbol{D}}^t = (\bar{D}^{(t)}_{a,b})$ for $t = 1, 2, \ldots$. Using induction with respect to $t = 1, 2, \ldots$, it can be shown that (67) extends to

$$\bar{D}^{(t)}_{ab} = \sum_{k,l \in \mathcal{I}_b} D^{(t)}_{ij,kl} \tag{88}$$

for any $i,j \in \mathcal{I}_a$. It follows from Perron Frobenius' Theorem that

$$\bar{\boldsymbol{D}}^t = \bar{\lambda}^t\bar{\boldsymbol{r}}\bar{\boldsymbol{\rho}} + o(\bar{\lambda}^t) \tag{89}$$

as $t \to \infty$, where $\bar{\lambda} = \lambda_{\max}(\bar{\boldsymbol{D}})$ is the largest eigenvalue of $\bar{\boldsymbol{D}}$, with corresponding $d \times 1$ right eigenvector $\bar{\boldsymbol{r}} = (r_a)$ and $1 \times d$ left eigenvector $\bar{\boldsymbol{\rho}} = (\rho_b)$. Comparing the lower part of (86) with (88) and (89), it follows that $\tilde{\lambda} = \bar{\lambda}$. To complete the proof, the leading right and left eigenvectors of $\boldsymbol{D}$ and $\bar{\boldsymbol{D}}$ can be normalized so that $\tilde{r}_{ij} = \bar{r}_a$ for any $ij \in \mathcal{I}_a$ and $\bar{\rho}_b = \sum_{kl \in \mathcal{I}_b} \tilde{\rho}_{kl}$. □

Subpopulation extinction. We will briefly indicate how some variables and recursions can be generalized to allow for subpopulation extinction. It is assumed in Section 3 that F_{tij}, H_{tij}, f_{tij} and h_{tij} are all undefined and assigned values NaN if at least one of i and j is extinct in generation t. Analogously, we put $A_{tij,kl} = \delta_{tij} = \text{NaN}$ if either $N_{ti} = 0$ or $N_{tj} = 0$, and $A_{tij,kl} = 0$ of none of i and j is extinct in generation t, but at least one of k and l is extinct in generation $t-1$. The recursions in (8) remain valid with these conventions, if all matrix multiplications ($\boldsymbol{A}_t\boldsymbol{h}_{t-1}$, $\boldsymbol{A}_t\boldsymbol{f}_{t-1}$ and $\boldsymbol{A}_t\boldsymbol{1}$) employ the rules $\text{NaN} + \text{NaN} = \text{NaN}$, $0 \cdot \text{NaN} = 0$ and $\text{NaN} \cdot C = \text{NaN}$ for $C > 0$. In particular, $\boldsymbol{h}_t$, $\boldsymbol{f}_t$, $\boldsymbol{A}_t\boldsymbol{h}_{t-1}$, $\boldsymbol{A}_t\boldsymbol{f}_{t-1}$ and $\boldsymbol{A}_t\boldsymbol{1}$ will have NaN components for those pairs i,j of subpopulations of which at least one is extinct in generation t. When these column vectors have been computed, we finally obtain the right hand sides of (8), using the conventions $\text{NaN} + \text{NaN} = \text{NaN}$, $C \cdot \text{NaN} = \text{NaN}$

and $C + \mathrm{NaN} = \mathrm{NaN}$ for *any* real-valued C, even $C = 0$. The conventions for $\boldsymbol{D}_t$ recursions are the same as for $\boldsymbol{A}_t$.

The subpopulation weights of Sections 3.3–3.4 may incorporate extinction through the rule $N_{ti} = 0 \Longrightarrow w_i = 0$, so that all extinct subpopulations are assigned zero weights. This implies in particular that quantities that depend on the weighting scheme, such as $F_{Tt}, F_{St}, H_{Tt}, G_{ST}, f_{Tt}, f_{St}, h_{Tt}$ and h_{St}, are well defined sums of terms, some of which satisfy $0 \cdot \mathrm{NaN} = 0$.

References

[1] F.W.Allendorf, G.Luikart, S.N.Aitken, Conservation and the Genetics of Populations, 2nd ed., Wiley-Blackwell, Chichester, UK, 2013.
[2] F.W.Allendorf, N.Ryman The role of genetics in population viability analysis, in: Population Viability Analysis, S.R.Bessinger, D.R.McCullogh (Eds.), The University of Chicago Press, Chicago, 2002.
[3] J.Backelin, The exact probability of identity by descent in the symmetric nearest neighbour stepping stone model on Z revisited, 2014, Manuscript.
[4] P.Beerli, Effect of unsampled populations on the estimation of population sizes and migration rates between sampled populations, Mol. Ecol. 13 (2004) 827–836.
[5] A.Bobbio, A.Horváth, M.Scarpa, M.Telek, Acyclic discrete phase type distributions: properties and a parameter estimation algorithm, Perform. Eval. 54 (2003) 1–32.
[6] P.Buchholz, Exact and ordinary lumpability in finite Markov chains, J. Appl. Prob. 31 (1994) 59–75.
[7] A.Caballero, Developments in the prediction of effective population size, Heredity 73 (1994) 657–679.
[8] A.Caballero, On the effective size of populations with separate sexes, with particular reference to sex-linked genes, Genetics 139 (1995) 1007–1011.
[9] D.Carmelli, L.L.Cavalli-Sforza, Some models of population structure and evolution, Theor. Popul. Biol. 9 (1976) 329–359.
[10] H.Caswell, Matrix Population Models, 2nd ed., Sinauer, Sunderland, MA, 2001.
[11] B.Charlesworth, Effective population size and patterns of molecular evolution and variation, Nat. Rev. Genet. 10 (2009) 195–205.
[12] R.K.Chesser, O.E.Rhodes, D.W.Sugg, A.Schnabel, Effective sizes for subdivided populations, Genetics 135 (1993) 1221–1232.
[13] S.C.Choy, B.S.Weir, Exact inbreeding coefficients in populations with overlapping generations, Genetics 89 (1978) 591–614.
[14] J.M.Cornuet, G.Luikart, Description and power analysis of two tests for detecting recent population bottlenecks from allele frequency data, Genetics 144 (1996) 2001–2014.
[15] D.R.Cox, H.D.Miller, The Theory of Stochastic Processes, Methuen & Co Ltd, London, 1965.
[16] J.F.Crow, Breeding structure of populations. II. Effective population number, in: Statistics and Mathematics in Biology, Iowas State Coll. Press, Ames, Iowa, 1954, pp. 543–556.
[17] J.F.Crow, C.Denniston, Inbreeding and variance effective population sizes, Evolution 42(3), (1988) 482–495.
[18] J.F.Crow, M.Kimura, An Introduction to Population Genetics Theory, The Blackburn Press, Caldwell, New Jersey, USA, 1970.
[19] R.Durrett, Probability Models for DNA Sequence Evolution, 2nd ed., Springer, New York, 2008.
[20] T.H.Emigh, The dynamics of finite haploid populations with overlapping generations. I. Moments, fixation, probabilities and stationary distributions, Genetics 92 (1979) 323–337.
[21] W.J.Ewens, On the concept of effective population size, Theor. Popul. Biol. 21 (1982) 373–378.
[22] W.J.Ewens, The effective population size in the presence of catastrophes, in: M.Feldman (Ed.), Mathematical Evolutionary Theory, Princeton University, Princeton, 1989, p. 9.
[23] W.J.Ewens, Mathematical Population Genetics. I. Theoretical Introduction, 2nd ed., Springer, New York, 2004.
[24] W.Feller, Diffusion processes in genetics, in: J.Neyman (Ed.) Proc. 2nd Berkeley Symp. on Math. Stat. Prob., University of California Press, Berkeley, 1951, pp. 227–246.
[25] J.Felsenstein, Inbreeding and variance effective numbers in populations with overlapping generations, Genetics 68 (1971) 581–597.
[26] J.Felsenstein, How can we infer geography and history from gene frequencies? J. Theor. Biol. 96 (1982) 9–20.
[27] I.R.Franklin, Evolutionary change in small populations, in: M.Soulé, B.Wilcox (Eds.), Conservation Biology: An Evolutionary-Ecological perspective, Sinauer Associates, Sunderland, Massachusetts, 1980, pp. 135–149.
[28] J.C.Garza, E.G.Williamson, Detection of reduction in population size using data from microsatellite loci, Mol. Ecol. 10(2) (2001) 305–318.
[29] M.M. Hansen, L.W. Andersen, J. Aspi, R. Fredrickson, Evaluation of the conservation genetic basis of management of grey wolves in Sweden. Swedish large carnivore inquiry. Publisher: Statens Offentliga Utredningar (The Swedish Government's Official Investigations), SOU 2011:37 (2011), Available from The Swedish Government, http://www.government.se (accessed September 2014).
[30] J.Hein, M.H.Schierup, C.Wiuf, Gene Genealogies, Variation and Evolution, A Primer in Coalescent Theory, Oxford University Press, Oxford, 2005.
[31] P.W.Hedrick, A standardized genetic differentiation measure, Evolution 59(3) (2005) 1633–1638.
[32] P.W.Hedrick, M.E.Gilpin, Genetic effective size of a meta-population. In I.A.Hanski, M.E.Gilpin (Eds.), Metapopulation Biology: Ecology, Genetics and Evolution, Academic Press, San Diego, 1996, pp. 165–181.
[33] H.M.Herbots, The structured coalescent, in: Progress in Population Genetics and Human Evolution, P.Donnelly, S.Tavaré (Eds.), Springer-Verlag, New York, 1997, pp. 231–255.
[34] O.Hössjer, Spatial autocorrelation for subdivided populations with invariant migration schemes, Methodol. Comput. Appl. Prob. 16(4) (2014) 777–810.
[35] O.Hössjer, On the eigenvalue effective size of structured populations. J. Math. Biol., 2014, available online, doi:10.1007/s00285-014-0832-5.
[36] O.Hössjer, N.Ryman, Quasi equilibrium, variance effective population size and fixation index for models with spatial structure, J. Math. Biol. 69(5) (2014) 1057–1128.
[37] P.Jorde, N.Ryman, Temporal allele frequency change and estimation of effective size in populations with overlapping generations, Genetics 139 (1995) 1077–1090.
[38] P.Jorde, N.Ryman, Unbiased estimator for genetic drift and effective population size, Genetics 177 (2007) 927–935.
[39] S.Karlin, Rares of approach to homozygosity for finite stochastic models with variable population size, Am. Nat. 102 (1968) 443–455.
[40] J.G.Kemeny, J.L.Snell, Finite Markov Chains, Springer, New York, 1976.
[41] M.Kimura, 'Stepping stone' model of population, Ann. Rep. Natl. Inst. Genet. Japan 3 (1953) 62–63.
[42] M.Kimura, Theoretical foundations of population genetics at the molecular level, Theor. Popul. Biol. 2 (1971) 174–208.
[43] M.Kimura, J.F.Crow, The measurement of the effective population number, Evolution 17 (1963) 279–288.
[44] M.Kimura, G.H.Weiss, The stepping stone model of population structure and the decrease of genetic correlation with distance, Genetics 61 (1964) 763–771.
[45] J.F.C.Kingman, The coalescent, Stoch. Proc. Appl. 13 (1982) 235–248.
[46] L.Laikre, Conservation genetics of Nordic carnivores: lessons from zoos, Hereditas 130 (1999) 203–216.
[47] L.Laikre, M.Jansson, F.W.Allendorf, S.Jakobsson and N.Ryman, Hunting effects on favourable conservation status of highly inbred Swedish wolves, Conserv. Biol. 27 (2013) 248–253.
[48] S.Leviyang, The distribution of F_{ST} for the island model in the large population, weak mutation limit, Stoch. Anal. Appl. 28 (2011) 577–601.
[49] S.Leviyang, The distribution of F_{ST} and other genetic statistics for a class of population structure models, J. Math. Biol. 62 (2011) 203–289.
[50] S.Leviyang, M.B.Hamilton, Properties of Weir and Cockerham's F_{ST} estimator and associated bootstrap confidence intervals, Theor. Popul. Biol. 79 (2011) 39–52.
[51] W.-H.Li, Effect of migration on genetic distance, Am. Nat. 110 (1976) 841–847.
[52] O.Liberg, H.Andrén, C.-H.Pedersen, H.Sand, D.Sejberg, P.Wabakken, M.Åkesson, S.Bensch, Severe inbreeding depression in a wild wolf Canis lupus population, Biol. Lett. 1 (2005) 17–20.
[53] L.-E.Liljelund, Predator Conservation Status, Interim report of the Predator Investigation SOU 2011:37, Governments Public Investigation, (in Swedish), pp. 134.
[54] G.Luikart, F.Allendorf, J.Cornuet, W.Sherwin, Distortion of allele frequency distributions provides a test for recent population bottlenecks, J. Hered. 89(3) (1998) 238–247.
[55] G.Luikart, N.Ryman, D.A.Tallmon, M.K.Schwartz, F.W.Allendorf, Estimation of census and effective population sizes: the increasing usefulness of DNA-based approaches, Conserv. Genet. 11 (2010) 355–373.
[56] G.Malécot, Un treatment stochastique des problemès linairés (mutation, linkage, migration) en géneétique de populations, Annales de l'Université de Lyon A 14 (1951) 79–117.
[57] G.Malécot, The Mathematics of Heredity, Freeman, San Francisco, 1969.
[58] T.Maruyama, On the rate of decrease of heterozygosity in circular stepping stone models of populations, Theor. Popul. Biol. 1 (1970) 101–119.
[59] T.Maruyama, Effective number of alleles in subdivided populations, Theor. Popul. Biol. 1 (1970) 273–306.
[60] T.Maruyama, P.A.Fuersti, Population bottlenecks and non equilibrium models in population genetics. II. Number of alleles in a small population that was formed by a recent bottleneck, Genetics 111 (1985) 675–689.
[61] T.Nagylaki, The strong migration limit in geographically structured populations, J. Math. Biol. 9 (1980) 101–114.
[62] T.Nagylaki, The inbreeding effective population number in dioecious populations, Genetics 139 (1995) 473–485.
[63] T.Nagylaki, Geographical invariance and the strong-migration limit in subdivided populations, J. Math. Biol. 41 (2000) 123–142.
[64] M.Nei, Analysis of gene diversity in subdivided populations, Proc. Natl. Acad. Sci. U.S.A. 70 (1973) 3321–3323.
[65] M.Nei, Molecular Population Genetics and Evolution, North-Holland, New York, 1975.
[66] M.Nei, *F*-statistics and analysis of gene diversity in subdivided populations, Ann. Hum. Genet. 41 (1977) 225–233.
[67] M.Nei, Molecular Evolutionary Genetics, Columbia University Press, 1987.
[68] M.Nei, A.Chakravarti, Y.Tateno, Mean and variance of F_{ST} in a finite number of incompletely isolated populations, Theor. Popul. Biol. 11 (1977) 291–306.
[69] M.Nei, F.Tajima, Genetic drift and estimation of effective population size, Genetics 98 (1981) 625–640.

[70] M.Nei, N.Takahata, Effective population size, gene diversity, and coalescence time in subdivided populations, J. Mol. Evol. 37 (1993) 240–244.
[71] M.F.Neuts, Matrix Geometric Solutions in Stochastic Models: Algorithmic Approach, Dover Publications, New York, 1995.
[72] M.Notohara, The coalescent and the genealogical process in geographically structured populations, J. Math. Biol. 29 (1990) 59–75.
[73] F.Olsson, O.Hössjer, L.Laikre, N.Ryman, Characteristics of the variance effective population size over time using an age structured model with variable size, Theor. Popul. Biol. 90 (2013) 91–103.
[74] F.Olsson, O.Hössjer, L.Laikre, N.Ryman, GESP – a program for genetic exploration of structured populations, 2014, Manuscript.
[75] F.Olsson, O.Hössjer, Estimation of the effective population size in age structured populations, 2014, Manuscript.
[76] M.E.Orrive, Effective population size in organisms with complex life-histories, Theor. Popul. Biol. 44 (1993) 316–340.
[77] E.Pollak, Effective population numbers and mean time to extinction in dioecious populations with overlapping generations, Math. Biosci. 52 (1980) 1–25.
[78] E.Pollak, A new method for estimating the effective population size from allele frequency changes, Genetics 104 (1983) 531–548.
[79] E.Pollak, Eigenvalue effective population numbers for populations that vary cyclically in size, Math. Biosci. 177, 178 (2002) 11–24.
[80] J.Räikkönen, J.A.Vucetich, L.M.Vucetich, R.O.Peterson, M.P.Nelson, What the inbred Scandinavian wolf population tells us about the nature of conservation, PLoS ONE 8(6) (2013) e67218, doi:10.1371/journal.pone.0067218.
[81] S.Rottenstreich, J.R.Miller, M.B.Hamilton, Steady state of homozygosity and G_{ST} for the island model, Theor. Popul. Biol. 72 (2007) 231–244.
[82] F.Rousset, Inbreeding and relatedness coefficients: what do they measure? Heredity 88 (2002) 371–380.
[83] N.Ryman, F.W.Allendorf, P.E.Jorde, L.Laikre, O.Hössjer, Samples from structured populations yield biased estimates of effective size that overestimate the rate of loss of genetic variation, Mol. Ecol. Resour. 14 (2014) 87–99.
[84] N.Ryman, O.Leimar, Effect of mutation on genetic differentiation among nonequilibrium populations, Evolution 62(9) (2008) 2250–2259.
[85] K.Y.Sampson, Structured coalescent with nonconservative migration, J. Appl. Prob. 43 (2006) 351–362.
[86] S.Sawyer, Results for the stepping stone model for migration in population genetics, Ann. Prob. 4 (1976) 699–728.
[87] S.Sawyer, J.Felsenstein, Isolation by distance in a hierarchically clustered population, J. Appl. Prob. 20 (1983) 1–10.
[88] P.Sjödin, I.Kaj, S.Krone, M.Lascoux, M.Nordborg, On the meaning and existence of an effective population size, Genetics 169 (2005) 1061–1070.
[89] M.Slatkin, Gene flow and genetic drift in a species subject to frequent local extinctions, Theor. Popul. Biol. 12 (1977) 253–262.
[90] M.Slatkin, Inbreeding coefficients and coalescence times, Genetical Research 58 (1991) 167–175.
[91] M.Slatkin, Seeing ghosts: the effect of unsampled populations on migration rate estimated for sampled populations, Mol. Ecol. 14 (2005) 67–73.
[92] M.Slatkin, L.Voelm, F_{ST} in a hierarchical model, Genetics 127 (1991) 627–629.
[93] M.E.Soulé (Ed.) Conservation Biology. The Science of Scarcity and Diversity, Sinauer Associates, Sunderland, Massachusetts, 1986.
[94] C.Strobeck, Average number of nucleotide differences in a sample from a single subpopulation: a test for subpopulation subdivision, Genetics 117 (1987) 149–153.
[95] J.A.Sved, B.D.H.Latter, Migration and mutation in stochastic models of gene frequency change, J. Math. Biol. 5 (1977) 61–73.
[96] L.W.Traill, B.W.Brook, R.R.Frankham, C.J.A.Bradshaw, Pragmatic population viability targets in a rapidly changing world, Biol. Conserv. 143 (2010) 28–34.
[97] J.Tufto, S.Engen, K.Hindar, Inferring patterns of migration from gene frequencies under equilibrium conditions, Genetics 144 (1996) 1911–1921.
[98] J.Tufto, K.Hindar, Effective size in management and conservation of subdivided populations, J. Theor. Popul. Biol. 222 (2003) 273–281.
[99] J.Wakeley, Segregating sites in Wright's island model, Theor. Popul. Biol. 53 (1998) 166–174.
[100] J.Wakeley, O.Sargsyan, Extensions of the coalescent effective population size, Genetics 181 (2009) 341–345.
[101] J.Wang, Effective size and *F*-statistics of subdivided populations. I. Monoecious species with partial selfing, Genetics 146, (1997) 1453–1463.
[102] J.Wang, Effective size and *F*-statistics of subdivided populations. II. Dioecious species, Genetics 146, (1997) 1465–1474.
[103] J.Wang, A.Caballero, Developments in predicting the effective size of subdivided populations, Heredity 82 (1999) 212–226.
[104] Y.Wang, E.Pollak, The effective number of a population that varies cyclically in size. I. Discrete generations, Math. Biosci. 166 (2000) 1–21.
[105] Y.Wang, E.Pollak, The effective number of a population that varies cyclically in size. II. Overlapping generations, Math. Biosci. 179 (2002) 161–181.
[106] R.S.Waples, A generalized approach for estimating effective population size from temporal changes in allele frequency, Genetics 121 (1989) 379–391.
[107] R.S.Waples, Definition and estimation of effective population size in the conservation of endangered species, in: Populations Viability Analysis, S.R.Beissinger, D.R.McCullogh (Eds.) The University of Chicago Press, Chicago, 2002.
[108] R.S.Waples, M.Yokota, Temporal estimates of effective population size in species with overlapping generations, Genetics 175 (2007) 219–233.
[109] G.H.Weiss, M.Kimura, A mathematical analysis of the stepping stone model of genetic correlation, J. Appl. Prob. 2 (1965) 129–149.
[110] M.C.Whitlock, N.H.Barton, The effective size of a subdivided population, Genetics 145 (1997) 427–441.
[111] M.C.Whitlock, D.E.McCauley, Some population genetic consequences of colony formation and extinction; genetic correlations within founding groups, Evolution 44 (1990) 1717–1724.
[112] H.M.Wilkinson-Herbots, Genealogy and subpopulation differentiation under various models of population structure, J. Math. Biol. 37 (1998) 535–585.
[113] S.Wright, Evolution in Mendelian populations, Genetics 16 (1931) 97–159.
[114] S.Wright, Size of population and breeding structure in relation to evolution, Science 87 (1938) 430–431.
[115] S.Wright, Isolation by distance, Genetics 28 (1943) 114–138.
[116] S.Wright, The genetical structure of populations, Ann. Eugen. 15 (1951) 323–354.